Published online 28 December 2012 *Nucleic Acids Research, 2013, Vol. 41, No. 3* ***1829–1847***
doi:10.1093/nar/gks1305

Sleeping Beauty transposon-based system for cellular reprogramming and targeted gene insertion in induced pluripotent stem cells

Ivana Grabundzija[1], Jichang Wang[1], Attila Sebe[2,3], Zsuzsanna Erdei[2], Robert Kajdi[4], Anantharam Devaraj[1], Doris Steinemann[5], Károly Szuhai[6], Ulrike Stein[1], Tobias Cantz[7], Axel Schambach[8], Christopher Baum[8], Zsuzsanna Izsvák[1,*], Balázs Sarkadi[2,*] and Zoltán Ivics[1,4,*]

[1]Max Delbrück Center for Molecular Medicine, Robert Rössle Strasse 10, 13125 Berlin, Germany, [2]Hungarian Academy of Sciences, Membrane Biology Research Group, Diószegi u. 64, 1113 Budapest, Hungary, [3]Department of Biochemistry and Molecular Biology, University of Debrecen, Egyetem tér 1, 4032, Debrecen, Hungary, [4]Division of Medical Biotechnology, Paul Ehrlich Institute, Paul Ehrlich Strasse 51-59, 63225 Langen, Germany, [5]Institute for Cellular and Molecular Pathology, Carl Neuberg Strasse 1, 30625 Hannover Medical School, Hannover, Germany, [6]Department of Molecular Cell Biology, Leiden University Medical Center, Einthovenweg 20, 2333 Leiden, The Netherlands, [7]Stem Cell Biology, Cluster-of-Excellence REBIRTH, Hannover Medical School, Carl Neuberg Strasse 1, 30625 Hannover, Germany and [8]Institute of Experimental Hematology, Hannover Medical School, Carl Neuberg Strasse 1, 30625 Hannover, Germany

Received June 21, 2012; Revised November 15, 2012; Accepted November 16, 2012

ABSTRACT

The discovery of direct cell reprogramming and induced pluripotent stem (iPS) cell technology opened up new avenues for the application of non-viral, transposon-based gene delivery systems. The *Sleeping Beauty* (SB) transposon is highly advanced for versatile genetic manipulations in mammalian cells. We established iPS cell reprogramming of mouse embryonic fibroblasts and human foreskin fibroblasts by transposition of OSKM (*Oct4*, *Sox2*, *Klf4* and *c-Myc*) and OSKML (OSKM + *Lin28*) expression cassettes mobilized by the *SB100X* hyperactive transposase. The efficiency of iPS cell derivation with SB transposon system was in the range of that obtained with retroviral vectors. Co-expression of the miRNA302/367 cluster together with OSKM significantly improved reprogramming efficiency and accelerated the temporal kinetics of reprogramming. The iPS cells displayed a stable karyotype, and hallmarks of pluripotency including expression of stem cell markers and the ability to differentiate into embryoid bodies *in vitro*. We demonstrate Cre recombinase-mediated exchange allowing simultaneous removal of the reprogramming cassette and targeted knock-in of an expression cassette of interest into the transposon-tagged locus in mouse iPS cells. This strategy would allow correction of a genetic defect by site-specific insertion of a therapeutic gene construct into 'safe harbor' sites in the genomes of autologous, patient-derived iPS cells.

INTRODUCTION

As a result of their plasticity and self-renewal capacity, human embryonic stem (ES) cells represent valuable tools for research and therapy, including tissue replacement following injuries or disease (1). However, there are several drawbacks involved with application of human ES cells, such as ethical issues concerning derivation of these cells from human embryos, and biological issues such as immune rejection once transplanted into incompatible recipients. To circumvent these problems, several methods have been proposed for the derivation of pluripotent cells from somatic cells including nuclear

*To whom correspondence should be addressed. Tel: +49 6103 77 6000; Fax: +49 6103 77 1280; Email: zoltan.ivics@pei.de
Correspondence may also be addressed to Zsuzsanna Izsvak. Tel: +49 30 9406 3510; Fax: +49 30 9406 2547; Email: zizsvak@mdc-berlin.de
Correspondence may also be addressed to Balazs Sarkadi. Tel: +36 1 372 4316; Fax: +36 1 372 4353; Email: balazs.sarkadi@biomembrane.hu

The authors wish it to be known that, in their opinion, the first three authors should be regarded as joint First Authors.

transplantation, cellular fusion and direct reprogramming by expression of pluripotency-related transcription factors. Direct reprogramming of differentiated somatic cells by gene transfer of a small number of defined transcription factors, namely *Oct4*, *Sox2*, *Klf4* and *c-Myc* (OSKM), has been shown to yield cells that are highly similar to ES cells in gene expression profiles, morphology, pluripotency and *in vitro* differentiation (2). In the mouse system, these induced pluripotent stem (iPS) cells have the ability to generate germline chimeras and mice fully derived from iPS cells following tetraploid complementation [reviewed in (3)]. In contrast to ES cells, iPS cells can be obtained from autologous, adult somatic cells, thereby obviating the need for prolonged immunosuppressive therapy in the context of cell transplantation. iPS cells can be genetically modified and can be coaxed to differentiate into endodermal, mesodermal and ectodermal cell types. Thus, the iPS cell technology offers a versatile and promising means for a variety of applications including modeling of monogenic and complex, multigenic traits and diseases, screens for drugs, cell differentiation, toxicology and autologous cell therapy (4–13). In one landmark study, iPS cells derived from fibroblasts of sickle cell anemia mice were genetically corrected by replacing the mutant β-globin allele with a wild-type allele by means of homologous recombination. This provided a source of iPS cells able to differentiate into disease-free hematopoietic precursors that cured the afflicted mice following transplantation (6).

The most widely applied methods for iPS cell reprogramming rely on the introduction of different combinations of transcription factors in the form of DNA, mRNA or protein into somatic cells. The early studies applied retroviral vectors for stable genomic insertion of the reprogramming genes (2,14,15). Oncogenicity of the factors used in reprogramming and the potential for insertional mutagenesis caused by integrating retroviral gene transfer vectors limit the value of the resulting iPS cells for clinical applications (16), and it is believed that avoiding multiple, permanent retroviral insertions will be a strict requirement for clinical translation of iPS cells. These concerns lead to the development of alternative approaches to reprogramming, including elimination of chromosomally integrated reprogramming genes from iPS cells by using Cre/lox or Flp technology (17–19), use of non-integrating gene transfer systems to deliver the reprogramming genes (20–22) and use of small-molecule chemicals in combination with genetic factors (23). For example, it was demonstrated that transient expression of the four key reprogramming factors using replication-incompetent adenoviral and Sendai viral vectors vectors can give rise to iPS cell lines (21,24,25). Similar, proof-of-concept for the applicability of Epstein-Barr Virus-derived oriP/EBNA1 episomal vector systems and transfection of plasmid constructs for the generation of iPS cells was recently obtained (20,22,26). Non-integrating reprogramming systems also include minicircle vectors (27), delivery of synthetic mRNAs encoding the reprogramming factors (28), transfection of miRNAs (29) and recombinant protein transduction (30,31). These important reports provide proof-of-concept for the generation of iPS cells without transgene integration, but at a >100-fold lower efficiency. Gradual reduction in reprogramming factor expression over a few days as the cells divide likely contributes to the low efficiency of non-integrating gene delivery systems, suggesting that prolonged (>10 days) expression of reprogramming factors is required for efficient reprogramming.

DNA transposons are discrete pieces of DNA with the ability to change their positions within the genome via a cut-and-paste mechanism called transposition. These mobile genetic elements can be harnessed as gene delivery vector systems that can be used as tools for versatile applications [for review, see (32)]. The paradigmatic use of any transposon-based vector system relies on transient expression of a transposase enzyme that enables genomic insertion of a gene of interest (GOI) flanked by terminal inverted repeats (TIRs) of the transposon (Figure 1A) [for review, see (32)]. In contrast to viral vectors, transposon vectors can be maintained and propagated as plasmid DNA, thereby providing simplicity and safety to the user. Because transposition proceeds through a cut-and-paste mechanism that only involves DNA, transposon vectors are not prone to incorporating mutations by reverse transcription (that are generated in retroviral stocks at reasonable frequencies), and can tolerate larger and more complex transgenes (33). *piggyBac* (PB) transposons have been shown to be applicable for iPS cell generation and, through repeated expression of the transposase in reprogrammed cells, the chromosomally integrated vector can be excised from the genome, thereby resulting in genetically 'clean' iPS cells (34,35). However, there are applications where the use of the other transposon systems could prove advantageous. The *Sleeping Beauty* (SB) transposon system (36) has several advantages over other transposon systems, including PB. First, transposition efficiency was greatly enhanced by the novel hyperactive *SB100X* transposase (37) that yields stable gene transfer efficiencies higher than that of PB (38) and comparable to those of integrating viral vectors, enabling highly efficient transgene integration and expression. Second, SB-based vectors are likely superior in safety because (i) SB shows a random genomic insertion profile without overt preference for integrating into genes and their transcriptional regulatory regions, whereas PB shows preferential integration into transcription units (38,39) and (ii) in comparison to PB transposons (40) the TIRs of SB vectors have negligible enhancer/promoter activity (41,42). Finally, as opposed to PB (43), there are no SB-related sequences in mammalian genomes, thereby precluding potential cross-mobilization between endogenous and exogenously introduced transposons.

We and others postulate that the ultimate therapeutic potential of iPS cells will be greatly enhanced by safe methods of genome engineering allowing targeted introduction of therapeutic gene cassettes (44). Here, we show iPS reprogramming of mouse embryonic fibroblasts (MEFs) and human foreskin fibroblasts (HFFs) by stable transposition of polycistronic OSKM and OSKML (also containing *Lin28*) expression cassettes mobilized by the *SB100X* transposase. The iPS cells

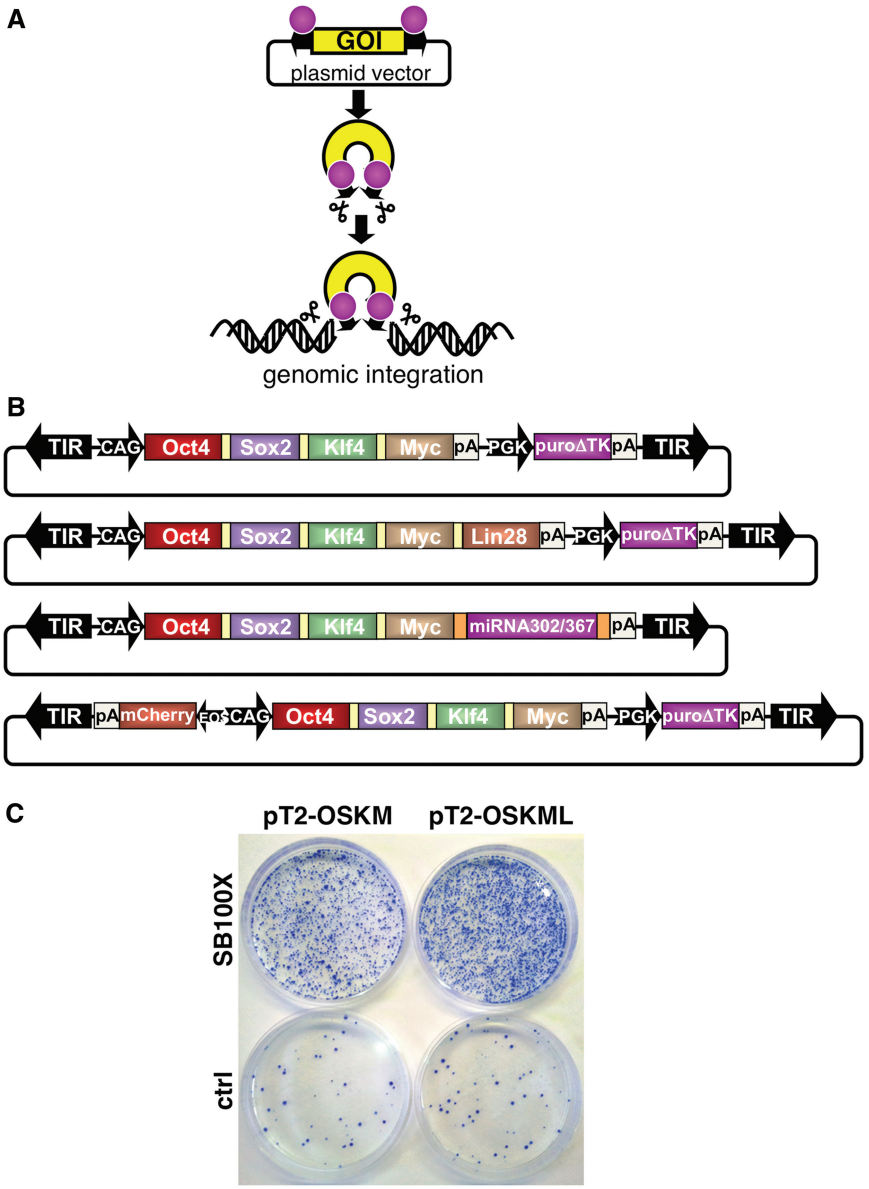

Figure 1. SB transposon-based vector system for iPS cell reprogramming. (**A**) The transposon is used as a bi-component vector system for delivering transgenes that are maintained in plasmids. One component contains a GOI between the transposon TIRs (black arrows), the other component is the transposase protein (pink spheres). The transposon is excised from the donor plasmid and is integrated at a chromosomal site by the transposase. (**B**) Schematic representation of SB transposon-based reprogramming vectors. Individual genes in four- and five-factor cassettes were linked by 2A self-cleaving peptide sequences and expressed from the CAG promoter. The miRNA302/367 cluster located in an intron is inserted in the reprogramming cassette. The pluripotency-reporting vector contains an EOS(3+)-mCherry pluripotency reporting cassette that consists of an ETn LTR coupled with a trimer of the Oct4 enhancer motif EOS(3+) driving the expression of *mCherry*. Black arrows represent SB transposon TIRs; bpA, bovine growth hormone polyadenylation signal; puΔtk, PGK promoter-driven puΔtk expression cassette. (**C**) Transposition of the four- and five-factor reprogramming transposons (pT2-OSKM and pT2-OSKML) in HeLa cells. In total, 2.5×10^5 cells were transfected with 500 ng of transposon-based reprogramming donor plasmids and 50 ng of transposase expression plasmids, placed under puromycin selection, and the resultant antibiotic-resistant colonies were stained.

show hallmarks of pluripotency, such as expression of stem cell markers and the ability to differentiate into embryoid bodies (EBs) *in vitro*. We demonstrate Cre recombinase-mediated exchange allowing simultaneous removal of the reprogramming cassette and targeted knock-in of an expression cassette of interest into the transposon insertion locus. We propose this novel approach of generating iPS cells as a viable and efficient alternative to other related methods.

MATERIALS AND METHODS

SB transposon-based reprogramming vectors

The CAG.OSKM-puΔtk and CAG.OSKML-puΔtk sequences containing the cDNAs of the open reading frames of the four Yamanaka factors (mouse *Oct4*, *Sox2*, *Klf4* and *Myc*) with or without *Lin28* were removed from PB vectors as described earlier (35) by NheI and NotI and cloned into the SpeI and NotI sites

of the pT2HB SB vector. Both resulting constructs contained a CAG-promoter driven reprogramming cassette [the reprogramming factors were combined into a single open reading frame separated by sequences encoding viral 2A peptides (45)], and a *puΔtk* cassette, flanked by SB inverted terminal repeats. The promoter-enhancer fragment EOS(3+) was cut out of the PL-SIN-EOS-C(3+)-EiP vector (46) with NcoI/MfeI and the fragment ends were blunted with Klenow polymerase. The EOS(3+) fragment was then cloned into the Klenow polymerase-treated AgeI site of pCAGGS-mCherry-C1Δ. The EOS(3+)-mCherry fragment was then cut out from the pEOS(3+)-mCherry-C1Δ plasmid with MluI/BamHI, and cloned into the MluI/BglII sites of the pT2-CAG.OSKM-puΔtk and pT2-CAG.OSKML-puΔtk plasmids. A DNA fragment containing the miRNA302/367 cluster was amplified from mouse genome by polymerase chain reaction (PCR) as described earlier (29). The amplified fragment was directly inserted between the reprogramming cassette and polyA sequence in the SB-based reprogramming vector pT2-OSKM.

Cell culture

HeLa cells were plated onto a six-well plate at a density of $\sim 2.5 \times 10^5$ cells per well 24 h prior to transfection. On the following day, the cells were co-transfected with 500 ng of transposon donor plasmids and 50 ng transposase expression plasmids, using FuGENE transfection reagent (Roche). To measure the transposition activity of these vectors in a colony-forming assay, the transfected cells were replated into 10-cm tissue culture dishes in 1:10 ratio 48 h post-transfection, and subjected to puromycin antibiotic selection.

Mouse OG2 MEFs were derived from OG2 mice (47) and cultured in mouse MEF medium: low glucose Dulbecco's Modified Eagle's medium (DMEM) without glutamine containing 10% fetal bovine serum (FBS) supplemented with 2 mM L-glutamine, 1 × nonessential amino acids, 0.1 mM 2-mercaptoethanol and 100 μg/ml primocin (InvivoGen). CF1-MEFs were grown in mouse MEF medium containing DMEM supplemented with 10% FBS, 1 × nonessential amino acids, 0.1 mM 2-mercaptoethanol and 100 μg/ml primocin. HFFs-1 were purchased from ATCC. Cells were cultured in DMEM (Invitrogen) supplemented with 10% FBS (Invitrogen) at 37°C under humidified atmosphere of air/CO_2 (19:1).

Mouse iPS cells were cultured in mouse iPS medium containing knockout DMEM with 15% FBS, 2 mM L-glutamine, 1 × nonessential amino acids, 0.1 mM 2-mercaptoethanol, 25 μg/ml L-ascorbic acid, 100 μg/ml primocin and purified recombinant leukemia inhibitory factor (LIF). Mouse iPS clones were maintained either on mytomicin-c-arrested feeders (CF1-MEFs) or on geltrex (1:200 dilution in F-12 DMEM). Human iPS cells were maintained on mitomycin C-treated MEF (CF-1) feeder cell layers (Millipore) in ESC medium: 80% KO-DMEM (Invitrogen) supplemented with 15% Serum Replacement, 1% nonessential amino acids (Invitrogen), 1 mM L-glutamine (Invitrogen), 0.1 mM beta-mercaptoethanol (Invitrogen) and 4 ng/ml human fibroblast growth factor (Invitrogen). Established iPS cells were passaged 1:2 every 72 h.

Reprogramming of MEFs using SB-based vectors

Twenty-four hours prior to electroporation OG2 cells were plated onto geltrex-coated six-well plates (2.5×10^5 cells per well). The next day cells were electroporated with the Neon™ transfection system (Invitrogen) according to the manufacturer's instructions. In each electroporation reaction, 5×10^5 cells were electroporated with 550 ng DNA [100, 250 or 500 ng of transposon vectors and 50 ng of CMV-SB100X vector expressing the enhanced *SB100X* transposase (37)]. Electroporation reactions were filled up to 550 ng DNA with pFV4a(CAT) plasmids. The conditions used for electroporation were 1350 V pulse voltage, 30 ms pulse width and one pulse. After the electroporation, each reaction was plated onto a geltrex-coated well of a six-well plate containing iPS medium. For the first 10 days medium was changed daily. Valproic acid (VPA) (Ergrnyl; Sanofi Aventis) was added to the iPS medium at 2 mM from day 2 until day 9 post-electroporation. Colonies were picked over days 14–20, trypsinized and plated onto feeders or geltrex-coated wells of a 24-well plate.

Generation of human iPS cells by SB transposons

HFF-1 cells (4×10^5 cells per well) were transfected by Nucleofection (Lonza) according to the manufacturer's instructions. In each transfection, 2 μg of transposon plasmid (pT2-OSKM or pT2-OSKML) and 0.2 μg of the CMV-SB100X vector were used. After transfection, the cells were plated onto Matrigel-coated (hES cell-qualified Matrix, BD Biosciences) six-well plates and were grown in MEF-conditioned ES medium. The medium was refreshed every day. Newly formed hiPS colonies were picked and transferred to Matrigel-coated 24-well plates, and expanded 4–6 days in MEF-conditioned ES medium. Cells were dissociated with trypsinization, plated onto feeder cells and cultivated in ES medium.

Recombinase-mediated cassette exchange

Mouse iPS cells (10^6) were resuspended in pre-warmed PBS after trypsinization, and centrifuged at 250 g for 5 min. The supernatant was aspirated and the recombination-mediated cassette exchange (RMCE)/CAG-mCherry plasmid was added to the cells, which were resuspended in Buffer R with gentle pipetting in a total volume of 110 μl. Cells were transfected with the Neon™ transfection system with the following settings: pulse voltage 1350 V, pulse width 30 ms and single pulse. The transfected cells were transferred into pre-warmed mouse iPS medium in a 10-cm feeder-coated dish. The cells were fed with fresh mouse iPS medium the next day and cultured for additional 2 days before FIAU (Moravek Biochemicals) selection (200 ng/ml). After selection for 2 weeks, surviving colonies that expressed *mCherry* were picked and expanded in 24-well plates.

In vitro differentiation assays

Undifferentiated, collagenase IV dissociated hiPSC were transferred to poly-2 hydroxyethyl-methacrylate (polyHEMA, Sigma-Aldrich) coated six-well plates. Cells were kept in suspension to generate EBs in EB medium consisting of 77.8% KO DMEM (Invitrogen), 20% ES tested FBS (Invitrogen), 1% nonessential amino acids (Invitrogen), 0.1 mM beta-mercaptoethanol (Invitrogen) and 1 mM L-glutamine (Invitrogen). EB medium was refreshed every day. Six days later EBs were placed onto gelatin-coated plates, the attached cells further differentiating spontaneously in DMEM supplemented with 10% ES tested FBS. Immunohistochemistry for or mRNA isolation was performed at the indicated times.

Immunohistochemistry and confocal microscopy

Mouse iPS cells were grown on inactivated MEFs in 12-well plates containing gelatinized (0.1% gelatine) glass cover slip inserts. To detect the expression of Sox2 and SSEA-1, immunostaining was performed with the ASC mES/iPS cell characterization kit (Applied StemCell) according to the manufacturer's instructions. To detect the expression of the Nanog, rabbit polyclonal anti-Nanog primary antibody (1:300) was used in conjunction with the ASC mES/iPS cell characterization kit. CF1-MEF cells were used as a negative and mouse E14 Tg2a ES cells as a positive control for the immunostainings.

Human iPS cells seeded onto eight-well Nunc Lab-Tek II Chambered Coverglass (Nalge Nunc International) were fixed with 4% paraformaldehyde (PFA) in Dulbecco's modified PBS (DPBS) for 30 min at room temperature. After DPBS washing steps, the samples were blocked for 1 h in DPBS containing 2 mg/ml bovine serum albumin, 1% fish gelatin, 5% goat serum and 0.1% Triton-X 100. Samples were then incubated for 1 h with primary antibodies. After extensive washes with DPBS, the corresponding fluorescently labeled secondary antibodies and DAPI (Invitrogen) for nuclear staining were added for another hour. Primary antibodies: anti-Oct4 (Santa Cruz Biotechnology), anti-Nanog (R&D Systems Inc), anti-SSEA4 (R&D Systems Inc), anti-podocalyxin (R&D Systems Inc), anti-α-fetoprotein (Sigma-Aldrich), anti-α-smooth muscle actin (Sigma-Aldrich) and anti-β-tubulin III (R&D Systems Inc). Alexa 488-labeled anti-mouse and Cy3-labeled anti-goat secondary antibodies were obtained from Jackson ImmunoResearch Laboratories. Samples were examined on an Olympus FV500-IX confocal laser scanning microscope.

Alkaline phosphatase staining

Cells were fixed with 4% formaldehyde in PBS for 30 min. Cells were then washed with PBS (3 × 5 min) and stained with BM Purple or BCIP®/NBT Liquid Substrate System (Sigma-Aldrich) for an hour at room temperature. CF1-MEF cells were used as a negative and mouse E14 Tg2a cells as a positive control.

Flow cytometry

Cells were washed once in PBS containing 0.5% bovine serum albumin and incubated for 30 min with different directly labeled anti-human antibodies: CD44-FITC, CD73-PE, CD90-PE (BD Pharmingen), PODXL-PE and SSEA4-APC (R&D Systems). In all samples, an anti-mouse Sca-1 (Ly-6A/E) (FITC or PE, BD Pharmingen) antibody was employed, for gating out the positively labeled mouse feeder cells. Samples were analyzed by a FACS-Calibur flow cytometer (Becton Dickinson Immunocytometry Systems) equipped with a 488-nm argon laser and a 635-nm red diode laser with CellQuest acquisition software (BDIS). iPS clones were obtained by cell sorting for SSEA4 positive cells using an Aria High Speed Cell Sorter (Beckton-Dickinson).

RT-PCR analysis

Embryoid bodies and human iPS cells were seperated from differentiated cells and from feeder cells using the Anti-TRA-1-60 MicroBead Kit (Miltenyi Biotec), and RNAs were extracted by using the RNAqueous-4PCR Kit (Ambion) following the instructions of the manufacturers. Total RNA (0.1 μg) was used for reverse transcription by using random hexamer primers from the Promega Reverse Transcription System Kit or with the High Capacity RNA-to-cDNA kit (Applied Biosystems). Quantitative RT-PCR was carried out using Taqman Gene Expression Master Mix (Applied Biosystems) and pre-designed TaqMan Gene Expression Assays (Applied Biosystems) on the StepOne Plus Real-Time PCR System (Applied Biosystems), according to the manufacturer's instructions and by using Power SYBR® Green PCR Master Mix (Applied Biosystems) on the ABI7900HT sequence detector (Applied Biosystems). All data were normalized to GAPDH expression.

Transcriptome profiling

For microarray analysis, quality-controlled DNA-free RNA samples to be hybridized on Illumina human-12 V4 expression BeadChips were processed using a linear amplification kit (Ambion) to generate biotin-labeled cRNA through 14 h of *in vitro* transcription. Purified cRNA was quality-checked on a 2100 Bioanalyzer (Agilent), and hybridized as recommended and using materials/reagents provided by the chip manufacturer.

Karyotyping

iPS cells were arrested with KaryoMAX Colcemid Solution (Invitrogen) for 30 min and harvested using trypsin-EDTA. Hypotonization was performed with prewarmed, 75 mM KCl. A 3:1 mixture of methanol and acetic acid was used for cell fixation. Slides were dropped and aged for 3 days. Samples were analyzed following trypsin banding and Giemsa staining on a Nikon Eclipse E600 microscope equipped with a COHU 4912 CCD camera. Karyotyping was performed using Applied Imaging MacKtype v5.6 software.

Transposon copy number analysis

Transposon copy numbers were determined by splinkerette PCR. Genomic DNA from the iPS clones was isolated with the GeneJET™ Genomic DNA Purification Kit according to the manufacturer's instructions, and 1 μg samples were digested with DpnII for 4 h. The samples were purified with the QIAquick PCR Purification Kit (Qiagen) according to the manufacturer's instructions, and ligated (150 ng) to MboI splinkerette adapters (25 pmol) in 20 μl reactions. Five microliters of the ligation reaction were used for the first PCR with primers Linker primer and T-Bal Rev with a cycle of 94°C for 3 min, followed by 15 cycles of 94°C for 30 s, 70°C for 30 s and 72°C for 30 s; 5 cycles of 94°C for 30 s, 63°C for 30 s and 72°C for 2 s with an increase of a 2 s per cycle; 5 cycles of 94°C for 30 s, 62°C for 30 s and 72°C for 12 s with an increase of 2 s per cycle; 5 cycles of 94°C for 30 s, 61°C for 30 s and 72°C for 22 s with an increase of 2 s per cycle and 5 cycles of 94°C for 30 s, 60°C for 30 s and 72°C for 30 s. Nested PCR was done with primers Nested and T-Bal with a cycle of 3 min at 94°C followed by 10 cycles of 94°C for 30 s, 65°C for 30 s and 72°C for 30 s and 20 cycles of 94°C for 30 s, 58°C for 30 s and 72°C for 30 s. The final elongation was performed for 5 min at 72°C.

Bisulfite sequencing

Bisulfite reactions were performed using the kit according to the manufacturer's instructions (Qiagen). Five microliter of bisulfite-treated genomic DNA was used in a standard PCR protocol to amplify the *Oct4* and *Nanog* promoter regions in mouse and human iPS cells and their parental fibroblasts (OG2 cells and HFF). PCR products were cloned into pGEM-T vectors (Promega) and sequenced using the M13 forward primer. Primers used to amplify the *Oct4* promoter region were described earlier (2).

Array-CGH analysis

Array-CGH was performed using the Agilent Mouse Genome Microarray Kit 244 k (Agilent Technologies, Santa Clara, CA, USA) high-resolution 60-mer oligonucleotide-based microarray with median overall probe spacing of ~10.9 kb. Labeling and hybridization of genomic DNA was performed according to the protocol provided by Agilent. Briefly, 0.75 μg of test DNA was labeled by random priming using the Agilent Genomic DNA Labeling Kit Plus, test DNA (mouse pre-RMCE and post-RMCE iPS cells) with Cy3-dUTP and reference DNA (mouse OG2 fibroblast) with Cy5-dUTP. Labeled products were purified by Amicon Ultra 30 k filters (Millipore, Billerica, MA, USA), combined and then mixed with mouse Cot-1 DNA (50 μg), Agilent 10× Blocking Agent and Agilent 2× Hybridization Buffer. This solution was hybridized to Agilent's 4 × 180 k Mouse Genome CGH microarray at 65°C with 20 rpm rotation for 24 h. Washing steps were performed according to the Agilent protocol. Microarray slides were scanned immediately using an Agilent microarray scanner at a resolution of 2 μm. For image analysis, default CGH settings of Feature Extraction Software (Agilent Technologies, Waldbronn, Germany) were applied. Output files from Feature Extraction were subsequently imported into Agilent's CGH data analysis software, DNA-Workbench. The Aberration Algorithm ADM2 was applied and Aberration Filters were set to threshold 15.0, at least four probes with mean $\log_2$ ratio of −0.5.

Histological analysis of EBs

Twenty-day-old human EBs were used for histological analysis, as previously described (48). EBs were briefly centrifuged at 800 rpm to remove the medium and subsequently coagulated by mixing with bovine plasma and thrombin (Sigma-Aldrich) at a ratio of 2:1. Formation of the clot containing ~30–40 EBs was followed by overnight fixation in 4% PFA. EBs were briefly rinsed in distilled water to remove PFA, dehydrated through a graded series of alcohol solutions (70–100%) and xylene, and embedded in paraffin for sectioning. Hematoxylin and eosin staining was performed on microscope slide-mounted, 0.3 μm sections by standard procedures. Images were obtained using a Zeiss AxioVision Rel. 4.8 imaging system and ×40/0.75 objective magnification.

RESULTS

Generation of mouse iPS cells by SB transposition

To explore the utility of the SB transposon as a reprogramming tool for the delivery of reprogramming genes into cells, two reprogramming vectors were constructed, containing either an OSKM or an OSKML (containing *Lin28* in addition to the OSKM factors) expression cassette driven by the constitutively active CAG promoter (Figure 1B) (35). The reprogramming factors were combined into a single reading frame with the help of 2 A self-cleaving peptide sequences. In addition, a puΔtk cassette allowing both positive (resistance to puromycin) and negative (sensitivity to gancyclovir) was also included in the SB transposon vectors (Figure 1B). Both SB reprogramming vectors were transpositionally active in human HeLa cells (Figure 1C). Next, we investigated cellular reprogramming in MEFs, by taking advantage of the OG2 transgenic line that expresses a GFP transgene driven by the *Oct4* promoter (49). Thus, MEFs isolated from OG2 embryos do not express GFP, but iPS cells derived from the MEFs do (due to activation of the *Oct4* promoter in pluripotent stem cells), which can be detected by fluorescent microscopy. The advantage of these genetically marked cells, therefore, lies in the possibility to monitor the reprogramming process.

About 5×10^5 early passage (P3) OG2-MEFs were electroporated with 100, 250 and 500 ng of transposon plasmids containing the reprogramming cassettes together with 50 ng of the *SB100X* transposase expression plasmid, and the cells were grown in the presence or absence of VPA that was shown to enhance the reprogramming process (23,50). In the presence of VPA, the first iPS-like colonies became visible between day 7

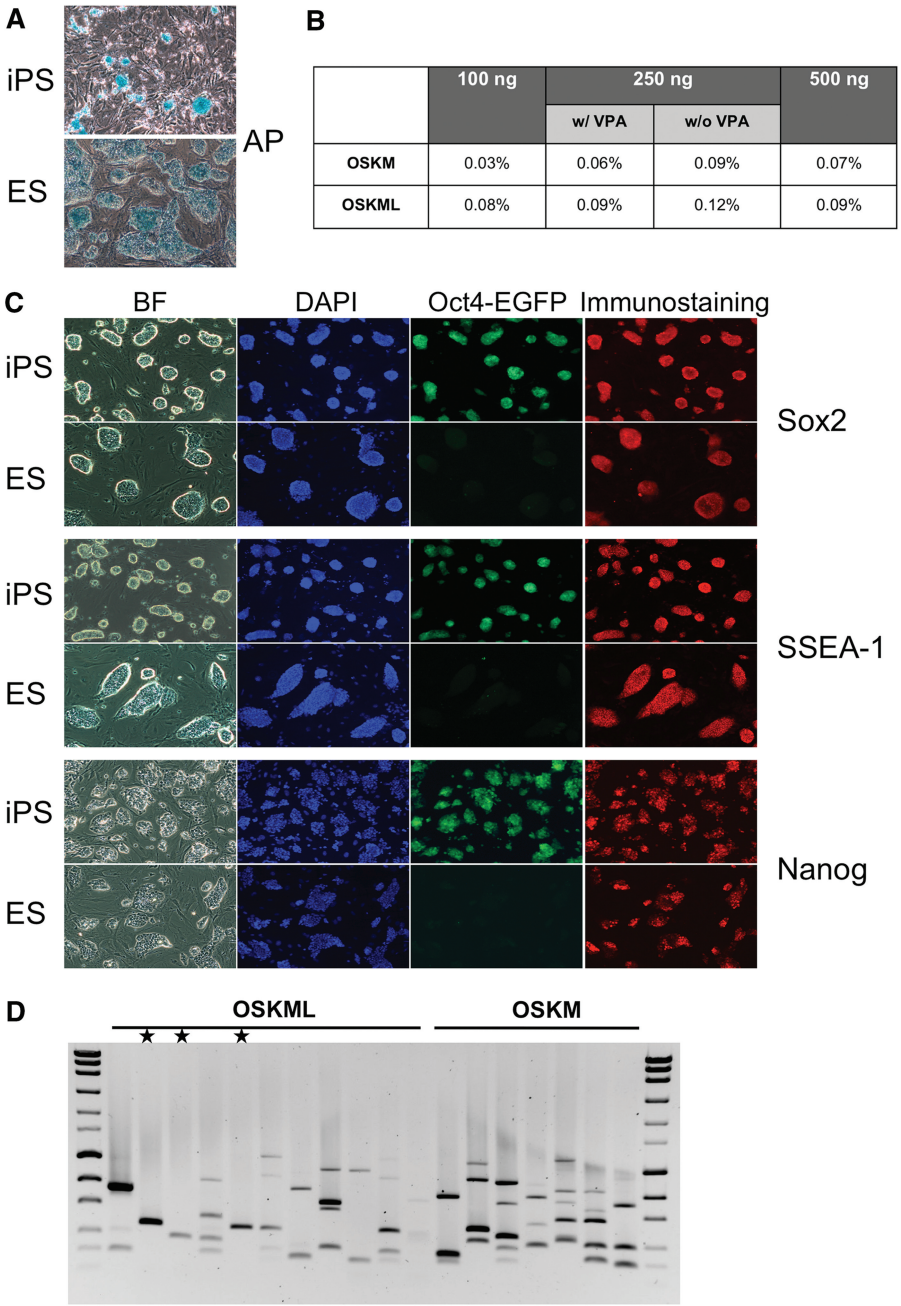

	100 ng	250 ng		500 ng
		w/ VPA	w/o VPA	
OSKM	0.03%	0.06%	0.09%	0.07%
OSKML	0.08%	0.09%	0.12%	0.09%

Figure 2. Characterization of mouse iPS clones generated with SB-based reprogramming vectors. (**A**) AP staining of iPS cell clones 24 days post-electroporation (top) and mouse ES cells (bottom). (**B**) iPS colony forming efficiencies of the pT2-OSKM and pT2-OSKML reprogramming vectors. A total of 100, 250 and 500 ng of transposon reprogramming vectors were electroporated together with 50 ng of the transposase expression plasmid pCSB100XNpA. At the 250 ng transposon dose, transfected cells were incubated in the presence or absence of VPA. (**C**) Immunostaining of Nanog, SSEA-1 and Sox2 in iPS cells at day 24 post-electroporation. Note that in addition to endogenously expressed Sox2, the antibody could have also reacted with exogenous Sox2 expressed from the reprogramming cassette. In addition, iPS cell clones generated from transgenic OG2-MEF cells express GFP from the endogenous Oct4-GFP locus. BF, bright field. (**D**) Transposon copy numbers in mouse iPS cells. iPS cell clones were generated by electroporation of $\sim 5 \times 10^5$ OG2-MEF cells with 100 ng of reprogramming transposon vectors and 50 ng of transposase expression vectors. Copy numbers of integrated OSKM and OSKML transposons were determined by splinkerette PCR; asterisks mark iPS cell clones with single-copy integrated transposons.

and 10, and green fluorescence could be observed several days later (around day 14, depending on the construct and the transfected plasmid amounts) (Figure 2). In the absence of VPA, colonies with a pre-iPS-like morphology started to form on day 3 post-electroporation, with GFP expression evident already at day 7.

As alkaline phosphatase (AP) is a stem cell membrane marker, and elevated expression of this enzyme is associated with an undifferentiated pluripotent stem cell state, the iPS cell colonies were stained for AP expression (Figure 2A), and counted to derive iPS reprogramming efficiencies. The highest numbers of AP-positive colonies

were obtained with electroporation of 250 ng of transposon and 50 ng of transposase plasmids (Figure 2B). Altogether, the OSKML SB vector was more efficient in iPS cell colony generation than the OSKM vector, and the increase in the reprogramming efficiency correlated with the increase in the amount of the reprogramming plasmids that were electroporated into the cells (Figure 2B). Consistent with earlier results showing a lack of enhancement of reprogramming by VPA in human and mouse fibroblasts following PB transposon-mediated gene transfer (35), colony formation was altogether higher in the absence of VPA (Figure 2B), but these iPS cell colonies displayed different morphology than those that grew in the presence of VPA. Generally, they were much larger than the VPA-treated colonies and more flat, lacking the typical spherical, clump-like morphology of murine ES cells. In addition, these colonies were positive for AP expression, but did not express GFP ubiquitously, but rather in smaller patches that seemed to be concentrated at areas of colonies showing increased cell division. Nevertheless, if these colonies were picked and passaged on feeder cells, their morphology changed to a typical ES-like state, and they started to express GFP ubiquitously (Supplementary Figure S1).

To investigate the pluripotency of these iPS cells, colonies with ES-like morphology were picked (mechanical picking followed by trypsinization of colonies), plated onto mouse feeder cells and subsequently used for AP- and immunostaining. In addition to the activation of the endogenous *Oct4* promoter, which was confirmed by green fluorescence of the reprogrammed cells, the iPS colonies also expressed endogenous pluripotency markers, including SSEA-1, Nanog and Sox2 (Figure 2C). The generated iPS colonies resembled in all instances mouse ES cell colonies that were used as a positive control for the immuno- and AP stainings, except for the expression of GFP that was specific for the OG2-transgenic cells (Figure 2C).

We investigated copy numbers of the integrated transposons by splinkerette-PCR. The iPS cell clones had transposon insertions in the range of 1–6 copies per clone (Figure 2D). Copy number was in general higher in OSKM-generated cells than in OSKML-generated cells (Figure 2D), consistent with either a higher transposition efficiency of the shorter OSKM transposon, or with higher gene dosage of the OSKM cassette required for iPS reprogramming. Importantly, ~10% of the colonies had a single-copy integration (Figure 2D), allowing subsequent engineering of the insertion locus.

Cre recombinase-mediated exchange of the reprogramming cassette in mouse iPS cells

Differentiation of iPS cells into various cell lineages requires removal of the reprogramming genes. However, because correction of genetic deficiencies may necessitate stable genomic insertion of therapeutic transgene cassettes in patient-derived cells, we reasoned that these two steps (removal of the reprogramming cassette and addition of a new expression cassette) could be achieved simultaneously by RMCE (Figure 3A). We previously developed a strategy for Cre recombinase-mediated RMCE in transgenic pig fibroblasts (51). In an analogous fashion, we flanked the OSKM cassette in the SB transposon vector by heterospecific *loxP* and *loxP257* recombination sites (Figure 3A). This vector was used to generate mouse iPS cells from OG2 fibroblasts, and a single-copy iPS cell line was employed for RMCE. The iPS cells were electroporated with two plasmids, one containing an *mCherry* marker cassette flanked by the *loxP* and *loxP257* sites and another transiently expressing Cre recombinase. RMCE yielded cells at an efficiency of ~0.01% that were resistant to FIAU due to loss of the TK marker in the reprogramming construct and that were red fluorescent due to genomic insertion of the *mCherry* expression cassette (Figure 3B). Genotyping of three individual iPS cell colonies with PCR primer pairs specific either to the reprogramming cassette or to transposon vector and *mCherry* sequences (Figure 3A) confirmed loss of the reprogramming cassette and gain of the *mCherry* cassette at the transposon-tagged genomic locus (Figure 3C).

Similar to their parental cells, the exchanged, reprogramming factor free iPS cells had an ES cell-like morphology, and expressed GFP from the *Oct4* promoter (Figure 3B), suggesting that they retained pluripotency. By means of high resolution array-CGH no chromosomal copy number alterations, deletions or duplications were identified in pre- or post-RMCE mouse iPS cells (Figure 3D). To investigate the DNA methylation status of the *Nanog* promoter, bisulfite sequencing on genomic DNAs isolated from parental and exchanged iPS cells and from OG2 fibroblasts was performed. As shown in Figure 3E, the promoter region of *Nanog* was demethylated in mouse iPS cells and methylated in OG2 fibroblasts, indicating that the epigenetic state of the *Nanog* gene was successfully reprogrammed from a transcriptionally repressed to an active state, and that this reprogrammed state was maintained in reprogramming factor-free iPS cells. To further characterize reprogramming factor-free mouse iPS cells on a molecular level, we determined the expression of mouse ES cell-specific genes. As shown in Figure 3F, these genes were highly expressed in parental as well as exchanged, reprogramming factor-free mouse iPS cells, as compared with OG2 fibroblasts.

The exchanged iPS cells formed EBs *in vitro*, and differentiated into the three germ layer lineages indicated by immunocytochemical stainings for the lineage markers α-SMA, β3-tubulin and Sox17 (Figure 4A). Consistent with the loss of pluripotency (and transcriptional deactivation of the *Oct4* promoter) during *in vitro* differentiation, the GFP signal disappeared in EBs derived from the exchanged iPS cells during the first week of culture (Figure 4A). Mouse iPS cell clones were subjected to gene expression (mRNA) analysis, and found to display upregulated expression of multiple, specific differentiation markers representing the three germ layers (Figure 4B). Taken together, RMCE allows removal of reprogramming genes and simultaneous knock-in of transgenes of interest at transposon-tagged loci in iPS cells that retain

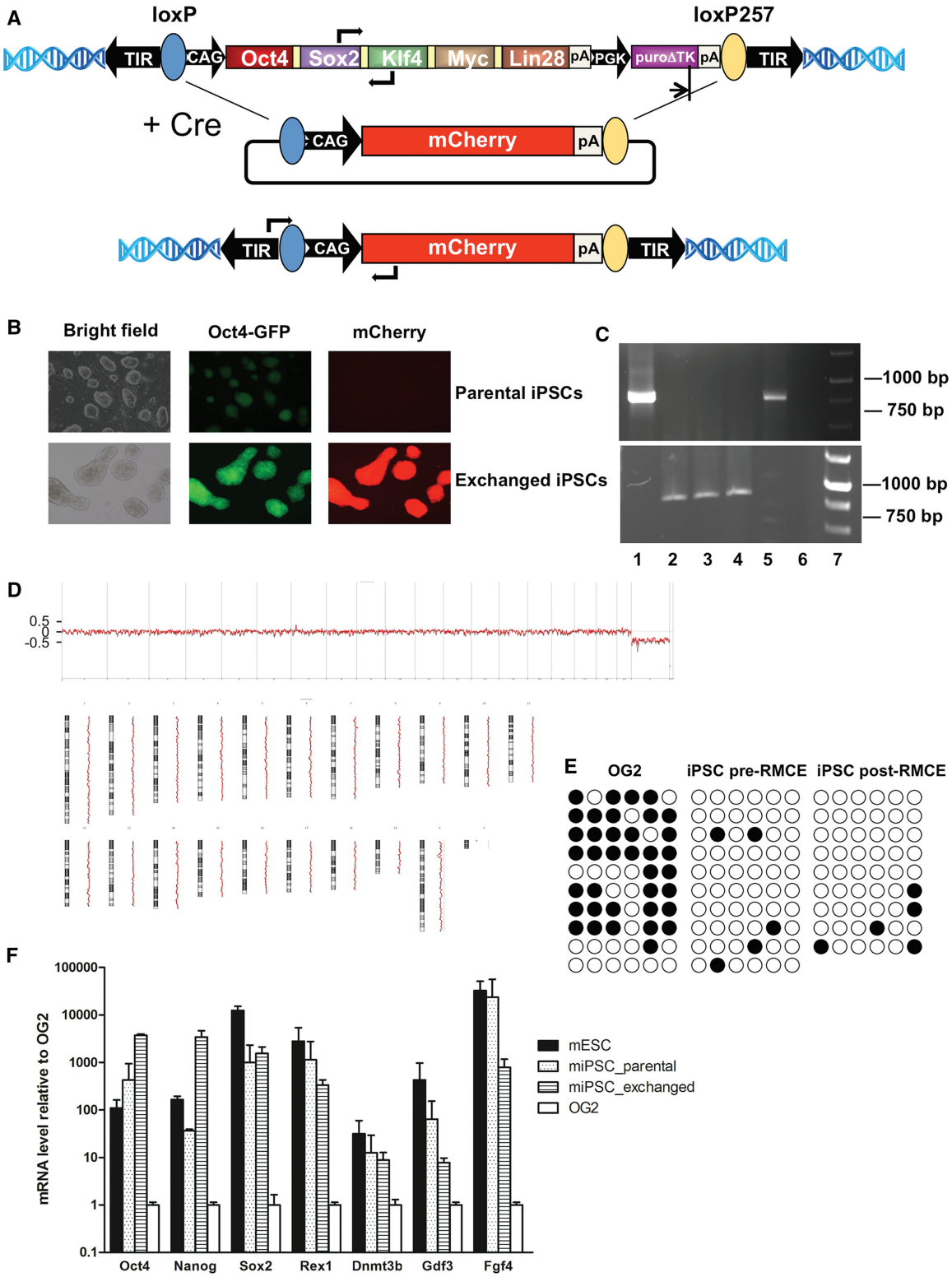

Figure 3. Cre recombinase-mediated cassette exchange in mouse iPS cells. (**A**) Schematic representation of RMCE. The OSKML expression cassette plus positive/negative selection cassette is flanked by heterospecific *loxP* sites alowing simultaneous removal of the reprogramming cassette from a genomically integrated, transposon-tagged locus and site-specific integration of an exogenously supplied transgene of interest also flanked by compatible *loxP* sites. RMCE is dependent on transient expression of Cre recombinase. (**B**) RMCE in mouse iPS cells. The OSKML factors plus selection genes were exchanged with *mCherry* in a single-copy mouse iPS clone following FIAU (200 nM) selection for 2 weeks. (**C**) Genomic PCR analysis of the exchanged iPS clone with primers shown in A, designed to detect the reprogramming cassette (top gel) and *mCherry* within a transposon vector (bottom gel). Lanes: (1) parental iPS clone, (2–5) iPS clones after RMCE and selection in FIAU, (6) OG-2 MEFs (negative control). The PCR products in lanes 2, 3 and 4 indicate that the reprogramming cassette was successfully exchanged with *mCherry*. (**D**) The genomic profiles of pre-RMCE (brown) and post-RMCE (red) mouse iPS cells by means of array-CGH (244 k, Agilent). Cy3/Cy5 ratios of each individual

(continued)

pluripotency in the absence of exogenous pluripotency factors.

SB-based pluripotency-reporting reprogramming vectors

Use of genetically engineered cells that can report reprogramming into a pluripotent state, such as the OG2 MEFs, is advantageous, since they can facilitate fast and easy identification of reprogrammed cells. However, the benefits of such cells are not available for the generation of autologous, patient-derived human iPS cells. To circumvent this limitation, we incorporated a pluripotency reporter cassette into the SB-based reprogramming vectors (Figure 1B). The pluripotency reporter cassette consisted of *mCherry* expressed from the strong LTR promoter of an Early Transposon (ETn) that is highly transcribed in ES cells (52) coupled with a trimer of Oct4 binding site. This promoter-enhancer combination is not active in differentiated cells, and was therefore specifically devised to mark pluripotent stem cells (46).

To investigate the activity of the modified reprogramming vectors, $\sim 5 \times 10^5$ early passage (P3) OG2-MEFs were electroporated with 500 ng of plasmids containing the reprogramming vectors together with 50 ng of the *SB100X* transposase expression plasmid. After electroporation, cells were plated into geltrex-coated six-well plates and grown in the absence of VPA. Cellular morphology began to change around day 3 post-transfection, and small pre-iPS colonies were visible as early as day 6. Red fluorescence could be observed around day 10 post-transfection in pre-iPS colonies, whereas GFP fluorescence appeared ~3–4 days later, as was previously observed by Hotta *et al.* (46). iPS colonies with ES cell-like morphology ubiquitously expressed both *mCherry* and GFP (Figure 5).

Generation of human iPS cells by SB transposition

To test the potential of the SB transposon-based system for iPS reprogramming in human cells, HFFs were electroporated with the reprogramming vectors (pT2-OSKM or pT2-OSKML or pT2-OSKM/EOS-mCherry) as described earlier. The first iPS-like colonies appeared 3 weeks after transfection, the first clumps being harvested 4 weeks after transfection (Figure 6A). *mCherry*-positive colonies generated with the OSKM/EOS-mCherry construct (Figure 5) appeared as early as day 6 (Figure 6A). The newly formed cells were morphologically indistinguishable from ES colonies (Figure 6B-D). As observed with the mouse cells, the presence of *Lin28* enhanced reprogramming: cells transfected with pT2-OSKML yielded more colonies, and the first signs of reprogramming appeared 1–2 days earlier. Furthermore, similar to mouse iPS cells, the majority of human iPS cell clones contained multiple transposon insertions in the range of 2–5 copies per cell (data not shown).

miRNAs have been reported to promote somatic cell reprogramming (29,53). To accelerate HFF reprogramming, we employed an SB-based reprogramming vector containing OSKM and the miRNA302/367 cluster (Figure 1B). ES-like colonies derived with this vector were observed within 6–7 days after transfection, 1 week earlier than with the OSKM vector, suggesting that the expression of miRNA302/367 improved the temporal kinetics of reprogramming (Figure 6A). The miRNA302/367 cluster improved reprogramming efficiency up to 15-fold compared with OSKM alone (Figure 6E).

iPS cell colonies were examined for markers of pluripotency. To investigate the DNA methylation status of the endogenous *Oct4* and *Nanog* promoters, bisulfite sequencing on genomic DNA samples isolated from human iPS cells and their parental HFF fibroblasts was performed. As shown in Figure 7A, the promoter regions of *Oct4* and *Nanog* were demethylated in human iPS cells and methylated in HFF fibroblasts, indicating that the epigenetic state of the *Oct4* and *Nanog* genes was successfully reprogrammed from a transcriptionally repressed to an active state. Human iPS cells uniformly expressed the pluripotency markers Oct4, Sox2, SSEA4, Tra-1-60, Tra-1-81 and AP as determined by immunocytochemistry, whereas the parental HFF cells were negative for these markers (Figure 7B). In addition, cells presented *de novo* expression of Nanog (Supplementary Figure S2A). Further analyses by confocal microscopy and by flow cytometry confirmed that iPS cells were positive for SSEA4 and podocalyxin (Supplementary Figure S2B–E). Human iPS cells and HFFs showed differential expression of CD44 and CD73 markers that are characteristic to more differentiated cellular phenotypes, and thus a decrease in their expression in iPS cells was expected and observed (Supplementary Figure S3). In addition, human iPS cell lines analyzed by quantitative RT-PCR (qRT-PCR) showed similar expression profiles of endogenous pluripotency genes compared with HES-3 (Figure 7C). Global transcriptome analyses further confirmed the induction of 26 important pluripotency-associated factors (Supplementary Figure S4). The dendogram (Figure 7D) and principal component analysis (Figure 7E) of these data sets showed that all human iPS cell lines clustered together, but were slightly different from a control data set of human ES cells (HuES6), consistent with earlier findings indicating that ES and iPS cells have similar, but not identical transcription profiles (54). Finally, karyotype analysis was done on one selected human iPS cell clone; these cells retained a

Figure 3. Continued
probe are plotted against the chromosomal localization from 1pter to y. Values around the baseline mean normal copy number state (2*n*), values above 0.5 mean a gain (3*n* or >), values below −0.5 mean mono-allelic loss (1*n*) and values below −3 mean bi-allelic loss. Copy number states are shown along each chromosome in more detail. The apparent loss of X chromosome is due to sex-mismatch hybridization. (**E**) DNA methylation of the *Nanog* promoter region analyzed by bisulfite sequencing. Open and closed circles indicate unmethylated and methylated CpG dinucleotides, respectively. (F) qRT-PCR analyses of mouse ES cell-specific genes in parental and exchanged, reprogramming factor-free mouse iPS cells. Expression levels of mouse ES cell-specific genes were normalized to *Gapdh,* and compared with levels in OG2 cells.

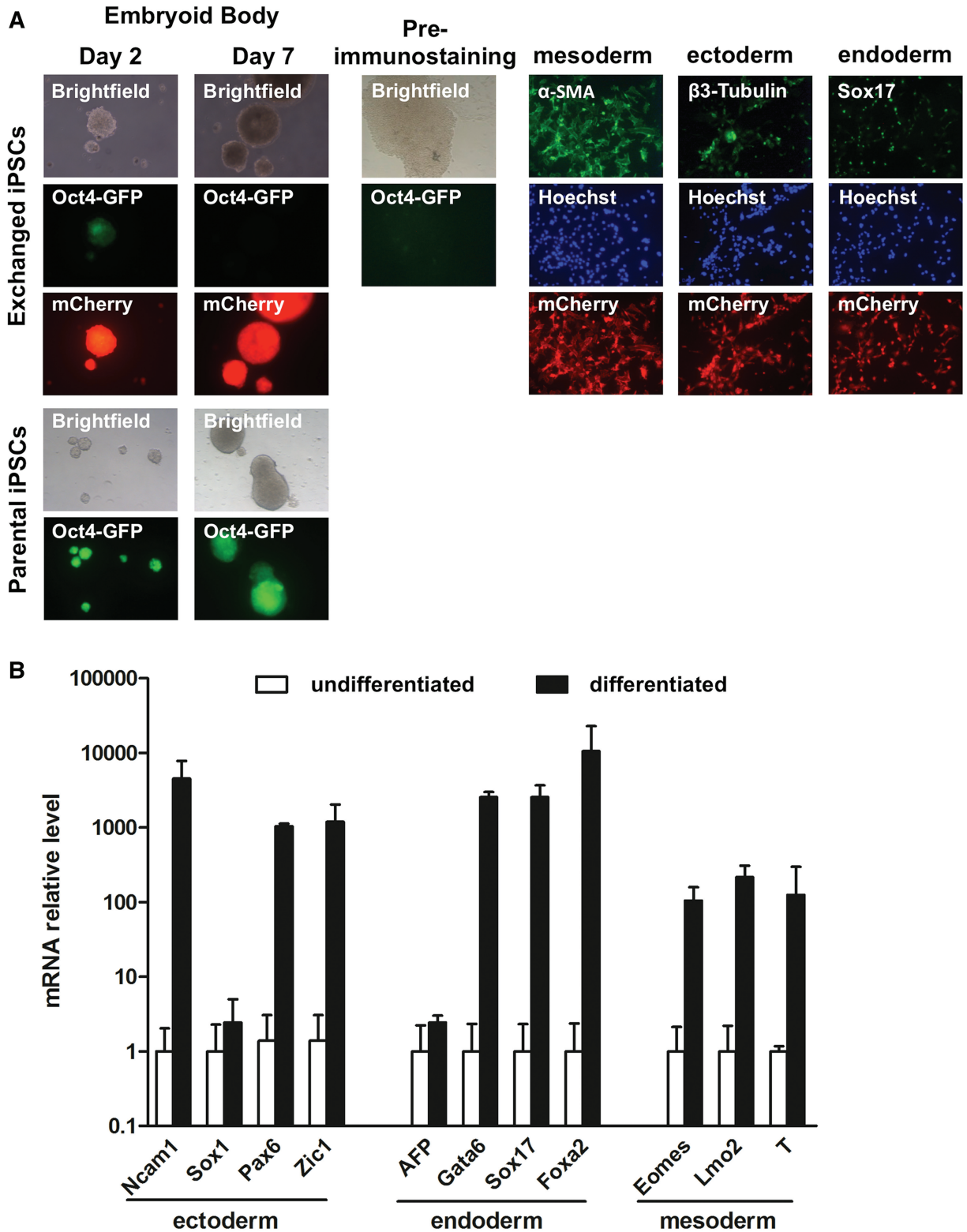

Figure 4. *In vitro* differentiation of exchanged mouse iPS cells into lineages from all three germ layers. (**A**) Immunostaining for α-SMA (mesoderm), β3-Tubulin (ectoderm) and Sox17 (endoderm) is shown. Oct4-GFP expression declines in EBs derived from exchanged iPS cells. (**B**) Multi-lineage differentiation of exchanged, reprogramming factor-free mouse iPS cells was determined by qPCR for markers of the three germ layer markers. Data are normalized to *Gapdh*, and relative to undifferentiated mouse iPS cells.

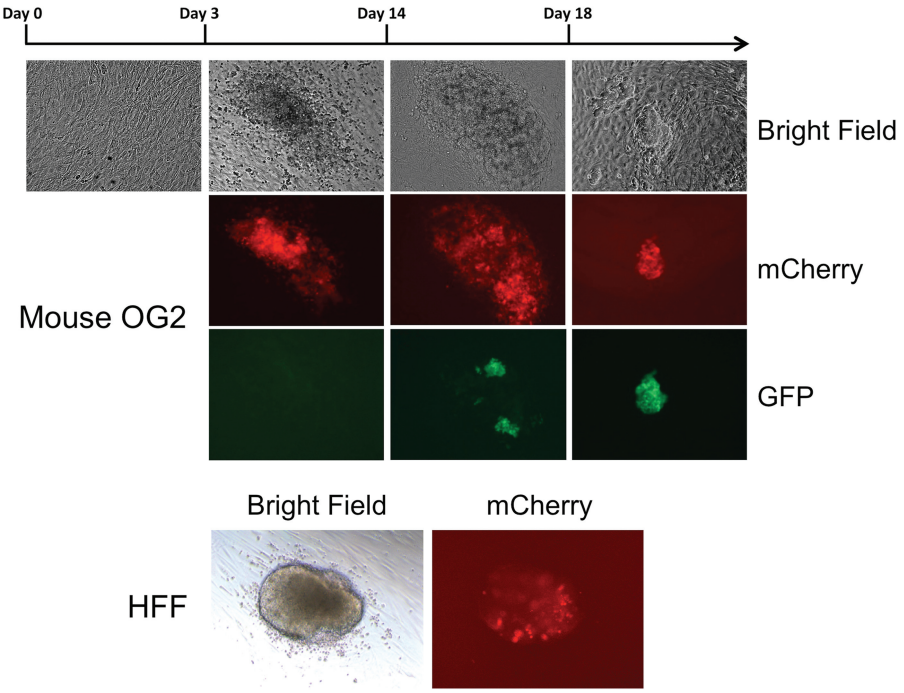

Figure 5. Generation of mouse and human iPS cells by SB transposon-based, pluripotency-reporting reprogramming vectors. Mouse and human iPS colonies were generated from OG2 MEFs and from HFFs, respectively. The resulting iPS cells express GFP from the *Oct4* promoter and *mCherry* from the EOS(3+) promoter. Human iPS cells express *mCherry* from the EOS(3+) promoter. A timeline of mouse iPS cell generation with the SB-based pluripotency reprogramming vector is shown. OG2 cells were electroporated with pT2-OSKML/EOS-mCherry and the *SB100X* transposase, and grown in mouse iPS medium in the absence of VPA. Cellular morphology began to change around day 3 post-transfection, and small pre-iPS colonies were visible as early as day 6. Around day 10 post-transfection pre-iPS colonies started to express the *mCherry* signal, while GFP fluorescence appeared several days later, around day 14. iPS clones with typical ES-like morphology and expressing both RFP and GFP fluorescence could be picked from day 18.

normal karyotype, irrespective of passage number (Figure 7F). Karyotyping by COBRA-FISH analysis on two additional clones indicated that >65% of the cells had a normal karyotype indistinguishable from that of the parental HFF cells (Supplementary Figure S5).

To investigate the transcriptional status of the reprogramming transgene construct in human iPS cells, expression of transgenes and endogenous pluripotency genes was determined by qRT-PCR (Supplementary Figure S6A). As previously seen with viral vector-derived human iPS cell lines, which sustain a low but detectable residual transgene expression (55,56), the SB-derived human iPS cells showed low expression of the reprogramming transgenes. In contrast, expression of endogenous Oct4 and Sox2 was consistently upregulated relative to the parental HFF cells. Unlike in mouse iPS cells, the *mCherry* signal was lost in human ES-like colonies after 3 weeks in culture, consistent with transgene silencing that was reversible by treating the cells with 5-Aza-2′-Deoxycytidine (5-Aza) (Supplementary Figure S6B).

Human iPS cells obtained by SB transposon-based reprogramming were subjected to *in vitro* differentiation studies by allowing them to form EBs (Figure 8A), which were assessed for expression of markers of the three germ layers. EBs were positive for alpha-fetoprotein (AFP) (endoderm), alpha-smooth muscle actin (α-SMA) (mesoderm) and betaIII-tubulin (ectoderm) as determined by immunocytochemistry (Figure 8B). Human iPS cell clones were subjected to gene expression (mRNA) analysis, and found to display upregulated expression of multiple, specific differentiation markers representing the three germ layers (Figure 8C). Expression of Oct4 and Nanog decreased, and expression of Pax6 increased (probably in parallel with the appearance of neuron-like cells) during differentiation, whereas HFFs were negative for these markers (Supplementary Figure S7). Expression of CAPG, a marker characteristic to skin cells, showed high initial expression in HFFs, and its expression declined in iPS or differentiated cells (Supplementary Figure S7).

In addition to expression of markers of germ layers, EBs can be used to demonstrate the differentiation potential of pluripotent stem cells by histological evidence of tissue-like structures that resemble early embryonic development (48). Thus, to further demonstrate functional pluripotency and differentiation potential of human iPS cells, we performed histological analysis of 20-day-old EBs. Hematoxylin- and eosin-stained EB sections were examined for morphological evidence of tissue differentiation. As shown in Figure 8D, tri-lineage differentiation was evidenced by the presence of neural rosettes (ectoderm), muscle fiber (mesoderm) and gut epithelium (endoderm) tissue-like structures characteristic for each of the three germ layers. Taken together, these data demonstrate that SB-derived human iPS cells were

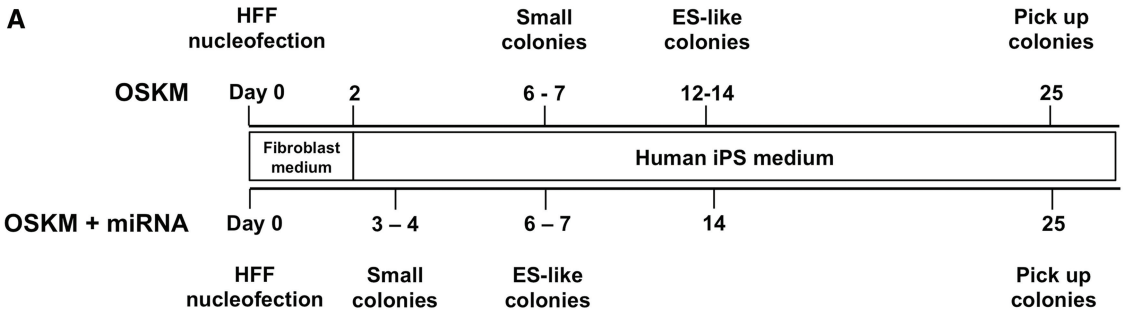

E

Reprogramming factors	Vector dose	Reprogramming efficiency
OSKM-mCherry	1 μg/ 2×10^5 cells	~ 0.07%
OSKM		~ 0.02%
OSKM-miRNA		~ 0.32%

Figure 6. Generation of human iPS cells with the SB reprogramming transposon system. (**A**) Timeline of SB-mediated iPS reprogramming. HFFs were electroporated with an SB transposon containing the reprogramming factors and the *SB100X* transposase. After electroporation, cells were seeded to one geltrex-coated well of a six-well plate. Cellular morphology began to change from day 4 post-transfection, and small colonies were formed as early as day 6. When the pluripotency-reporting transposon vector was used, *mCherry*-positive ES-like colonies formed ~2 weeks post-transfection, allowing real-time monitoring of the formation of human iPS cells. The miRNA302/367 promoted apparence of small colonies and ES-like colonies at 2 days and 1 week post-electroporation, respectively, earlier than OSKM. iPS colonies were picked after 3 weeks. (**B**) Confluent HFF cells grow in monolayers showing a typical fibroblast morphology. (**C**) Three to four weeks after transfection with transposons containing the reprogramming cassettes colonies were formed, which were picked and expanded. (**D**) Morphology of established human iPS cell line shows ES and iPS cell-like characteristics when grown on feeder cells. (**E**) iPS colony forming efficiencies of reprogramming vectors. Colonies were stained with AP and counted 3 weeks after transfection.

reprogrammed to pluripotency, and closely recapitulated the functional properties of human ES cells.

DISCUSSION

The advantage of SB transposon-based gene delivery is that it combines the favorable features of viral vectors with those of naked DNA molecules. Namely, owing to permanent genomic insertion of transgene constructs (Figure 1A), transposition-mediated gene delivery can lead to sustained and efficient transgene expression both *in vitro* (37,57) and in preclinical animal models (58). The recent development of the *SB100X* hyperactive transposase (37) allows efficient stable gene transfer following non-viral gene delivery into therapeutically relevant primary cell types, including stem or progenitor cells. For example, the use of the *SB100X* system yielded robust gene transfer efficiencies into human hematopoietic progenitors (37,57), mesenchymal stem cells, muscle stem/progenitor cells (myoblasts), iPS cells (59) and T cells (60). These cells are relevant targets for stem cell biology and for regenerative medicine and gene- and cell-based therapies of complex genetic diseases.

Here, we demonstrated the applicability of the SB transposon system for the efficient generation of iPS cells from both mouse and human fibroblasts. The efficiency of iPS cell derivation with SB transposon vectors approaches that obtained with MLV-derived retroviral vectors expressing each of the four factors separately (~0.1% in MEFs and ~0.01% in human fibroblasts) [reviewed in (4)]. The OSKML vectors were more efficient in iPS reprogramming than the OSKM vectors (Figure 2A). It was demonstrated earlier that ectopic expression of *Lin28* can accelerate iPS cell formation that is directly proportional to the cell division rate [reviewed in (3)]. This effect of *Lin28* on increased cell proliferation could amplify the number of target cells, in which each daughter cell has an independent probability of becoming an iPS cell, while the elevated rates of DNA replication may be a necessary prerequisite for epigenetic changes such as DNA and histone modifications to occur and allow the transition to pluripotency [reviewed in (3)]. In addition, it was suggested recently by Wang and coworkers that transcriptional reactivation of *Oct4* target genes might be a rate-limiting step in the conversion of somatic cells to pluripotent cells (61). Since it is known that *Lin28* facilitates the expression of *Oct4* in human ES cells at the post-transcriptional level (62), it is possible that elevated levels of *Oct4* induce faster activation of *Oct4* targets, thereby facilitating the reprogramming process.

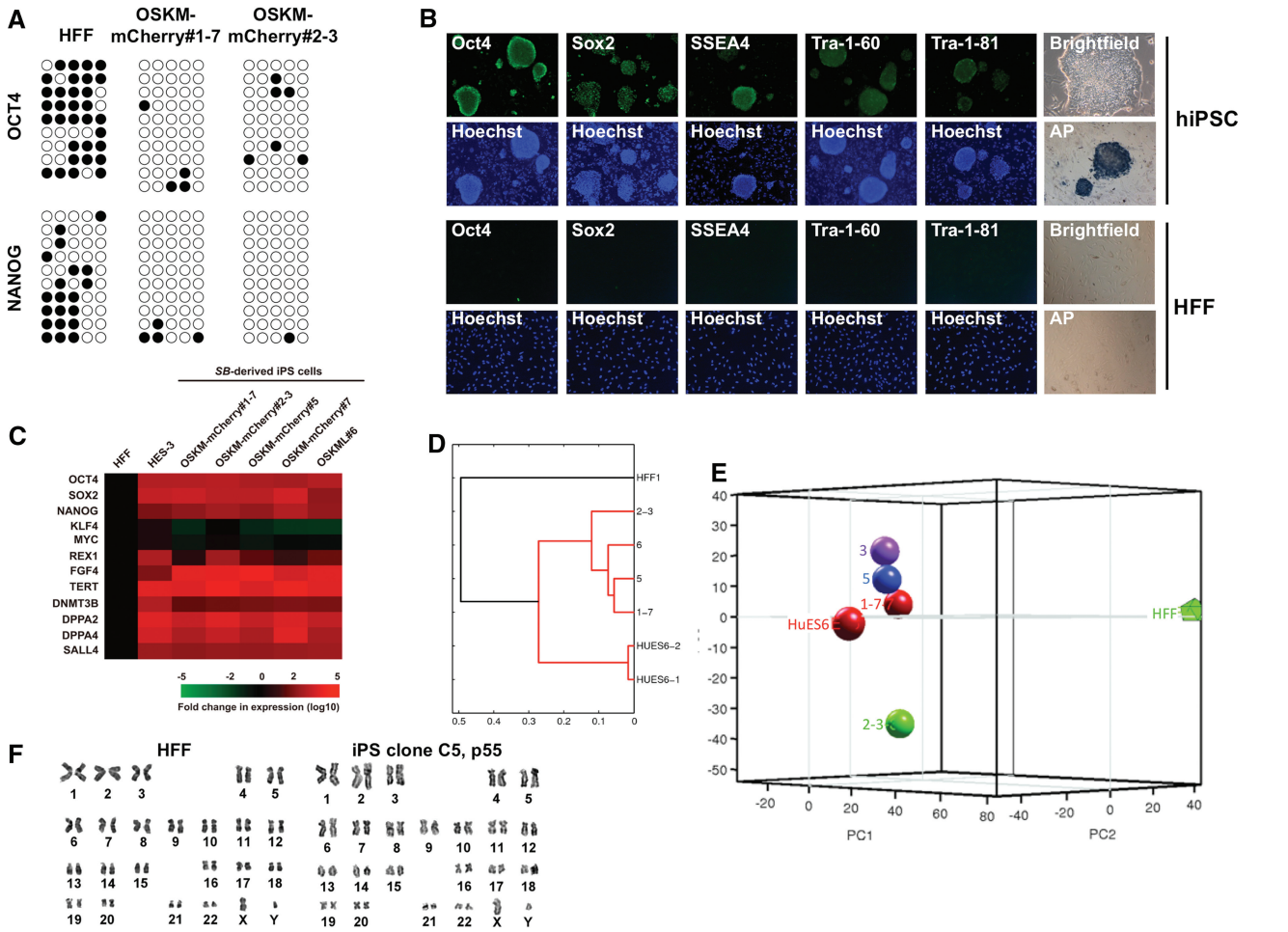

Figure 7. Characterization of human iPS cells. (**A**) DNA methylation of the promoter regions of the *Oct4* and *Nanog* genes analyzed by bisulfite sequencing. Open and closed circles indicate unmethylated and methylated CpG dinucleotides, respectively. (**B**) Immunostaining for Oct4, Sox2, SSEA4, Tra-1-60 and Tra-1-81 in human iPS cells as well as AP staining show expression of pluripotency markers. (**C**) Heat map showing similar expression profiles of pluripotency genes in human iPS cells and the human ES cell line HES-3, as determined by qRT-PCR. Data were normalized against *Gapdh*, and relative to HFF. (**D**) Dendogram and (**E**) principal component analysis depicting the transcriptome profiles of the human iPS cell lines 1–7, 2–3, 5 and 6 in comparison to a set of human ES cells (HuES6) and parental fibroblasts (HFF). (**F**) Karyotype analysis of human iPS cells. Human iPS cells of clone C5 retained normal karyotypes after 55 passages.

It was reported earlier that the addition of VPA to the cells during reprogramming enhanced the reprogramming efficiency of mouse and human fibroblasts (23,50). However, this effect was observed neither in earlier studies with PB reprogramming vectors (35) nor here with SB vectors. Namely, we observed an increase in reprogramming efficiency and kinetics in the absence of VPA. However, even though the iPS cell colonies generated in the absence of VPA were AP-positive, they did not express *Oct4* promoter-driven GFP ubiquitously, and had a characteristically different cellular morphology. Yusa *et al*. observed a dramatic growth suppression of the un-reprogrammed colonies by VPA, noting that even though the partially reprogrammed colonies contained Nanog-positive patches or subcolonies where reprogramming apparently did occur, the surrounding un-reprogrammed cells prevented reprogrammed cells from expanding and forming ES cell-like colonies (35). Therefore, passaging and trypsinization could act to 'free' such reprogrammed subcolonies from un-reprogrammed neighbor cells, and facilitate their further growth, as observed here.

In this study, we also created SB-based pluripotency-reporting reprogramming vectors by incorporating an EOS(3+) promoter-enhancer sequence-driven *mCherry* fluorescence marker in the OSKM and OSKML reprogramming vectors. This pluripotency-reporting cassette was more sensitive than the endogenous *Oct4*-GFP reporter cassette: iPS cells emitted red fluorescence at an earlier time point and with higher expression than the *Oct4*-GFP cassette, as was previously reported by Hotta *et al*. (46). The sensitivity and the high expression of the pluripotency marker gene makes these reprogramming vectors very useful for detecting reprogrammed patches or subcolonies of partially reprogrammed clones in cultures obtained with low amounts of reprogramming vectors, or in cells that are difficult to reprogram, which could then be picked and passaged to obtain completely reprogrammed colonies.

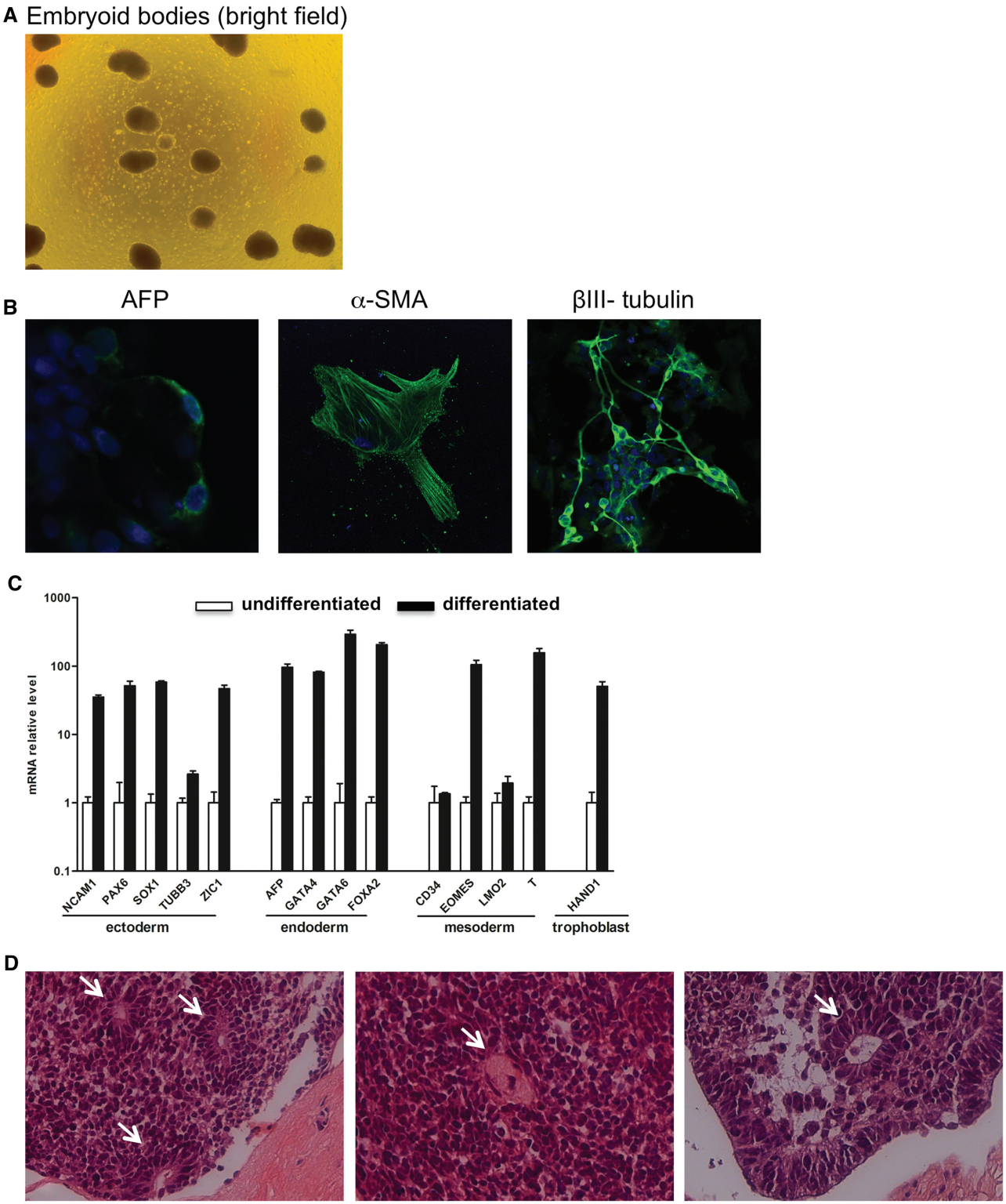

Figure 8. EB-mediated differentiation of human iPS cells. (**A**) iPS cells were kept in suspension on polyHEMA-coated six-well plates in EB medium to allow formation of cystic EBs for 6 days. (**B**) After 6 days, EBs were placed onto gelatin-coated plates, and the spontaneously differentiating, attached cells were assessed for markers of the three germ layers. Cells were positive for the endodermal marker AFP, the mesodermal marker α-SMA and the ectodermal marker βIII-tubulin. (**C**) Multi-lineage differentiation of human iPS cells was determined by qPCR for markers of the three germ layer markers, and compared with undifferentiated human iPS cells. Data are normalized to *Gapdh*, and relative to undifferentiated human iPS cells. (**D**) Histological evidence of EB germ layer differentiation. Shown are images of hematoxylin- and eosin-stained histological sections of EBs obtained from human iPS cells. Tri-lineage differentiation potential is evidenced by the presence of structures characteristic to ectodermal (neural rosettes, left), mesodermal (muscle fiber, middle) and endodermal (gut epithelium, right) tissues, indicated by arrows.

We demonstrated that the efficiency of reprogramming can be increased by increasing the amounts of the transposon reprogramming vectors electroporated into the cells. This suggests that it might be possible to further improve the efficiency of SB-mediated reprogramming by further increasing the amounts of the electroporated reprogramming vectors. However, in light of our analysis of transposon copy numbers in iPS colonies, such a strategy may prove counter-productive. Namely, transposon copy number analysis in the iPS clones revealed that even at reduced transposon vector doses the majority of iPS clones contained multiple (at least 2) transposon insertions. As earlier studies have shown that it is relatively straightforward to generate single-copy insertions in HeLa cells by titrating the transposon components in the transfection reactions (37,38), these results suggest selection for >1 copies during iPS cell reprogramming, which might be limited by the levels of expression of the reprogramming factors. Two papers have demonstrated that the quick reactivation of the endogenous *Oct4* gene is a crucial step in the reprogramming process (29,61), and that the fusion of *Oct4*, *Sox2* and *Nanog* to the transcriptional transactivation domain of herpes simplex virus protein VP16 can dramatically increase reprogramming speed and efficiency (61). This discovery indicates that by improving the efficiency of the reprogramming vectors by using such high-performance engineered factors or by increasing reprogramming factor expression by codon optimization and additional elements incorporated in the transgene cassette design (63), it might be possible to generate single-copy iPS cell clones more efficiently.

It has been shown previously that miRNAs are essential regulators of cell fate and pluripotency and play important role in somatic cell reprogramming (53,64–67). Recent studies have demonstrated that the miRNA cluster 302/367 promotes generation of human iPS cells (53), and can drive efficient somatic cell reprogramming even in the absence of the exogenous reprogramming factors (29). In agreement with those findings, addition of the miRNA cluster 302/367 to our pT2-OSKM reprogramming vector resulted in ~15-fold improvement in the efficiency of human iPS cell generation. However, in the mouse system we did not observe a similar positive effect on the generation of iPS cells. In addition, the morphology of mouse iPS colonies generated with the pT2-OSKM-miR-302/367 vector resembled that of epiblast stem cells (EpiSCs) (68–70), and was distinct from the morphology of the ES cell-like iPS clones generated with pT2-OSKM and pT2-OSKML vectors (Supplementary Figure S8). This observation could be explained in light of miRNA expression profiles in both ES- and EpiSCs indicating that those two pluripotent states have distinct miRNA signatures (71). According to the latest reports, a 'naïve' pluripotent state compatible with the inner cell mass and early epiblast is represented by murine ES cells that predominantly express the miR-290/295 cluster, whereas a 'primed' pluripotent state, similar to the post-implantation epiblast and represented by murine EpiSCs and human ES cells, predominantly expresses the miR-302/376 cluster (64,71). In this manner, use of the pT2-OSKM-miR-302/376 vector in our reprogramming experiments could have shifted the balance in the mouse system from generation of the typical iPS colonies with an ES cell-like morphology toward the derivation of cells resembling EpiSCs, which are characterized by the high expression of miR-302/362 cluster (71).

A major goal of human cell-based therapy is to develop methods that allow treatment of patients afflicted with genetic and degenerative disorders with a ready supply of defined transplantable cells. Because of their plasticity and unlimited capacity for self-renewal, human iPS cells have been proposed for use in 'personalized' cell-based therapies. Targeted genetic manipulation of stem cells is well advanced, and offers the opportunity to correct monogenic, life-threatening genetic defects. For such purposes it would be necessary to deliver and stably integrate a therapeutic gene construct into the genomes of autologous, patient-derived iPS cells, followed by differentiation into a linage of interest and transplantation of genetically corrected ('healed') cells. Such protocols will be especially justified in conditions, where autologous, patient-derived target cells are scarce and/or not amenable to genetic correction by *ex vivo* technologies. For example, Fanconi anemia (FA) patients with an advanced bone marrow failure have almost no hematopoietic stem cells (HSCs) in their hematopoietic tissues, precluding a classic HSC-based *ex vivo* gene therapy.

In a gene therapy setup, an SB transposon vector could carry both a reprogramming cassette flanked by homospecific *loxP* sites and a therapeutic cassette. After reprogramming has taken place, the reprogramming cassette could be excised by Cre recombinase-mediated excision. In another scenario, the SB transposon could deliver the reprogramming cassette flanked by heterospecific *loxP* sites. Following generation of iPS cells, the reprogramming cassette could be exchanged via Cre recombinase-mediated exchange with a therapeutic gene construct that is also flanked by the same recombination sites. We demonstrated the applicability of the latter strategy by site-directed integration of a fluorescent marker into a transposon-tagged locus (Figure 3). This strategy would allow phenotype correction and reprogramming in a single step. This would be especially important in FA, because it has been previously shown that phenotype correction is required for iPS reprogramming in FA fibroblasts (5). For a therapeutic application, it will be important that the therapeutic transgene cassette is inserted into a 'safe harbor' locus to avoid genotoxic effects and unwanted phenotypes. From the currently applied integrating vector systems, the SB transposon is especially noteworthy for its lack of preference for inserting into genes (39). The reprogramming SB transposon was integrated into a TA site on chromosome X in the mouse iPS cells that were subsequently used for RMCE (Supplementary Figure S9). Importantly, there are no known protein coding and miRNA genes in a window of ±20 kb around the transposon insertion site. This provides proof-of-concept for the generation of iPS cells with a single SB transposon integrated into a 'safe harbor' chromosomal locus. The establishment of safe protocols for the generation and clonal tracking of iPS cells by

rational genome engineering along with advanced differentiation protocols of iPS cells would open the field for potential correction of a multitude of severe monogenetic or acquired disorders of hematopoiesis, including aplastic anemias, immunodeficiencies, storage disorders, infecious diseases such as HIV infection and certain forms of cancer.

SUPPLEMENTARY DATA

Supplementary Data are available at NAR Online: Supplementary Figures 1–9 and Supplementary Methods.

ACKNOWLEDGEMENTS

We thank A. Bradley for kindly providing PB-based OSKM and OSKML expression vectors. The technical support toward some of the experiments provided by A. Apati, T. Orban, A. Kozma, D. de Jong and C. Voss is hereby gratefully acknowledged. We thank M. Arauzo-Bravo for his support in analyzing the data of human iPS cell transcriptomes. We appreciate support and advice from A. Nagy throughout the project.

FUNDING

EU FP7 [PERSIST, 222878; InduStem, 230675], Hungarian stem cell project [TÁMOP-4.2.2-08/1-2008-0015], Hungarian Research Fund (OTKA) [NK83533] and grants from the Deutsche Forschungsgemeinschaft 'Mechanisms of gene vector entry and persistence' [SPP1230, IV 21/4-2]; Bundesministerium für Bildung und Forschung [ReGene, 01GN1003A]. Funding for open access charge: Institutional funds.

Conflict of interest statement. None declared.

REFERENCES

1. Shao,L. and Wu,W.S. (2010) Gene-delivery systems for iPS cell generation. *Expert Opin. Biol. Ther.*, **10**, 231–242.
2. Takahashi,K. and Yamanaka,S. (2006) Induction of pluripotent stem cells from mouse embryonic and adult fibroblast cultures by defined factors. *Cell*, **126**, 663–676.
3. Hanna,J.H., Saha,K. and Jaenisch,R. (2010) Pluripotency and cellular reprogramming: facts, hypotheses, unresolved issues. *Cell*, **143**, 508–525.
4. Gonzalez,F., Boue,S. and Izpisua Belmonte,J.C. (2011) Methods for making induced pluripotent stem cells: reprogramming a la carte. *Nat. Rev. Genet.*, **12**, 231–242.
5. Raya,A., Rodriguez-Piza,I., Guenechea,G., Vassena,R., Navarro,S., Barrero,M.J., Consiglio,A., Castella,M., Rio,P., Sleep,E. *et al.* (2009) Disease-corrected haematopoietic progenitors from Fanconi anaemia induced pluripotent stem cells. *Nature*, **460**, 53–59.
6. Hanna,J., Wernig,M., Markoulaki,S., Sun,C.W., Meissner,A., Cassady,J.P., Beard,C., Brambrink,T., Wu,L.C., Townes,T.M. *et al.* (2007) Treatment of sickle cell anemia mouse model with iPS cells generated from autologous skin. *Science*, **318**, 1920–1923.
7. Park,I.H., Arora,N., Huo,H., Maherali,N., Ahfeldt,T., Shimamura,A., Lensch,M.W., Cowan,C., Hochedlinger,K. and Daley,G.Q. (2008) Disease-specific induced pluripotent stem cells. *Cell*, **134**, 877–886.
8. Xu,D., Alipio,Z., Fink,L.M., Adcock,D.M., Yang,J., Ward,D.C. and Ma,Y. (2009) Phenotypic correction of murine hemophilia A using an iPS cell-based therapy. *Proc. Natl Acad. Sci. USA*, **106**, 808–813.
9. Amabile,G. and Meissner,A. (2009) Induced pluripotent stem cells: current progress and potential for regenerative medicine. *Trends Mol. Med.*, **15**, 59–68.
10. Ye,L., Chang,J.C., Lin,C., Sun,X., Yu,J. and Kan,Y.W. (2009) Induced pluripotent stem cells offer new approach to therapy in thalassemia and sickle cell anemia and option in prenatal diagnosis in genetic diseases. *Proc. Natl Acad. Sci. USA*, **106**, 9826–9830.
11. Ye,Z., Zhan,H., Mali,P., Dowey,S., Williams,D.M., Jang,Y.Y., Dang,C.V., Spivak,J.L., Moliterno,A.R. and Cheng,L. (2009) Human-induced pluripotent stem cells from blood cells of healthy donors and patients with acquired blood disorders. *Blood*, **114**, 5473–5480.
12. Zou,J., Maeder,M.L., Mali,P., Pruett-Miller,S.M., Thibodeau-Beganny,S., Chou,B.K., Chen,G., Ye,Z., Park,I.H., Daley,G.Q. *et al.* (2009) Gene targeting of a disease-related gene in human induced pluripotent stem and embryonic stem cells. *Cell Stem Cell*, **5**, 97–110.
13. Wernig,M., Zhao,J.P., Pruszak,J., Hedlund,E., Fu,D., Soldner,F., Broccoli,V., Constantine-Paton,M., Isacson,O. and Jaenisch,R. (2008) Neurons derived from reprogrammed fibroblasts functionally integrate into the fetal brain and improve symptoms of rats with Parkinson's disease. *Proc. Natl Acad. Sci. USA*, **105**, 5856–5861.
14. Aoi,T., Yae,K., Nakagawa,M., Ichisaka,T., Okita,K., Takahashi,K., Chiba,T. and Yamanaka,S. (2008) Generation of pluripotent stem cells from adult mouse liver and stomach cells. *Science*, **321**, 699–702.
15. Sommer,C.A., Stadtfeld,M., Murphy,G.J., Hochedlinger,K., Kotton,D.N. and Mostoslavsky,G. (2009) Induced pluripotent stem cell generation using a single lentiviral stem cell cassette. *Stem Cells*, **27**, 543–549.
16. Okita,K., Ichisaka,T. and Yamanaka,S. (2007) Generation of germline-competent induced pluripotent stem cells. *Nature*, **448**, 313–317.
17. Kaji,K., Norrby,K., Paca,A., Mileikovsky,M., Mohseni,P. and Woltjen,K. (2009) Virus-free induction of pluripotency and subsequent excision of reprogramming factors. *Nature*, **458**, 771–775.
18. Soldner,F., Hockemeyer,D., Beard,C., Gao,Q., Bell,G.W., Cook,E.G., Hargus,G., Blak,A., Cooper,O., Mitalipova,M. *et al.* (2009) Parkinson's disease patient-derived induced pluripotent stem cells free of viral reprogramming factors. *Cell*, **136**, 964–977.
19. Voelkel,C., Galla,M., Maetzig,T., Warlich,E., Kuehle,J., Zychlinski,D., Bode,J., Cantz,T., Schambach,A. and Baum,C. (2010) Protein transduction from retroviral Gag precursors. *Proc. Natl Acad. Sci. USA*, **107**, 7805–7810.
20. Okita,K., Nakagawa,M., Hyenjong,H., Ichisaka,T. and Yamanaka,S. (2008) Generation of mouse induced pluripotent stem cells without viral vectors. *Science*, **322**, 949–953.
21. Stadtfeld,M., Nagaya,M., Utikal,J., Weir,G. and Hochedlinger,K. (2008) Induced pluripotent stem cells generated without viral integration. *Science*, **322**, 945–949.
22. Gonzalez,F., Barragan Monasterio,M., Tiscornia,G., Montserrat Pulido,N., Vassena,R., Batlle Morera,L., Rodriguez Piza,I. and Izpisua Belmonte,J.C. (2009) Generation of mouse-induced pluripotent stem cells by transient expression of a single nonviral polycistronic vector. *Proc. Natl Acad. Sci. USA*, **106**, 8918–8922.
23. Huangfu,D., Osafune,K., Maehr,R., Guo,W., Eijkelenboom,A., Chen,S., Muhlestein,W. and Melton,D.A. (2008) Induction of pluripotent stem cells from primary human fibroblasts with only Oct4 and Sox2. *Nat. Biotechnol.*, **26**, 1269–1275.
24. Fusaki,N., Ban,H., Nishiyama,A., Saeki,K. and Hasegawa,M. (2009) Efficient induction of transgene-free human pluripotent stem cells using a vector based on Sendai virus, an RNA virus that does not integrate into the host genome. *Proc. Jpn. Acad. Ser. B Phys. Biol. Sci.*, **85**, 348–362.
25. Seki,T., Yuasa,S., Oda,M., Egashira,T., Yae,K., Kusumoto,D., Nakata,H., Tohyama,S., Hashimoto,H., Kodaira,M. *et al.* (2010) Generation of induced pluripotent stem cells from human

terminally differentiated circulating T cells. *Cell Stem Cell*, **7**, 11–14.
26. Yu,J., Hu,K., Smuga-Otto,K., Tian,S., Stewart,R., Slukvin,I.I. and Thomson,J.A. (2009) Human induced pluripotent stem cells free of vector and transgene sequences. *Science*, **324**, 797–801.
27. Jia,F., Wilson,K.D., Sun,N., Gupta,D.M., Huang,M., Li,Z., Panetta,N.J., Chen,Z.Y., Robbins,R.C., Kay,M.A. *et al.* (2010) A nonviral minicircle vector for deriving human iPS cells. *Nat. Methods*, **7**, 197–199.
28. Warren,L., Manos,P.D., Ahfeldt,T., Loh,Y.H., Li,H., Lau,F., Ebina,W., Mandal,P.K., Smith,Z.D., Meissner,A. *et al.* (2010) Highly efficient reprogramming to pluripotency and directed differentiation of human cells with synthetic modified mRNA. *Cell Stem Cell*, **7**, 618–630.
29. Anokye-Danso,F., Trivedi,C.M., Juhr,D., Gupta,M., Cui,Z., Tian,Y., Zhang,Y., Yang,W., Gruber,P.J., Epstein,J.A. *et al.* (2011) Highly efficient miRNA-mediated reprogramming of mouse and human somatic cells to pluripotency. *Cell Stem Cell*, **8**, 376–388.
30. Zhou,H., Wu,S., Joo,J.Y., Zhu,S., Han,D.W., Lin,T., Trauger,S., Bien,G., Yao,S., Zhu,Y. *et al.* (2009) Generation of induced pluripotent stem cells using recombinant proteins. *Cell Stem Cell*, **4**, 381–384.
31. Kim,D., Kim,C.H., Moon,J.I., Chung,Y.G., Chang,M.Y., Han,B.S., Ko,S., Yang,E., Cha,K.Y., Lanza,R. *et al.* (2009) Generation of human induced pluripotent stem cells by direct delivery of reprogramming proteins. *Cell Stem Cell*, **4**, 472–476.
32. Ivics,Z., Li,M.A., Mates,L., Boeke,J.D., Nagy,A., Bradley,A. and Izsvak,Z. (2009) Transposon-mediated genome manipulation in vertebrates. *Nat. Methods*, **6**, 415–422.
33. Zayed,H., Izsvak,Z., Walisko,O. and Ivics,Z. (2004) Development of hyperactive sleeping beauty transposon vectors by mutational analysis. *Mol. Ther.*, **9**, 292–304.
34. Woltjen,K., Michael,I.P., Mohseni,P., Desai,R., Mileikovsky,M., Hamalainen,R., Cowling,R., Wang,W., Liu,P., Gertsenstein,M. *et al.* (2009) piggyBac transposition reprograms fibroblasts to induced pluripotent stem cells. *Nature*, **458**, 766–770.
35. Yusa,K., Rad,R., Takeda,J. and Bradley,A. (2009) Generation of transgene-free induced pluripotent mouse stem cells by the piggyBac transposon. *Nat. Methods*, **6**, 363–369.
36. Ivics,Z., Hackett,P.B., Plasterk,R.H. and Izsvak,Z. (1997) Molecular reconstruction of Sleeping Beauty, a Tc1-like transposon from fish, and its transposition in human cells. *Cell*, **91**, 501–510.
37. Mates,L., Chuah,M.K., Belay,E., Jerchow,B., Manoj,N., Acosta-Sanchez,A., Grzela,D.P., Schmitt,A., Becker,K., Matrai,J. *et al.* (2009) Molecular evolution of a novel hyperactive Sleeping Beauty transposase enables robust stable gene transfer in vertebrates. *Nat. Genet.*, **41**, 753–761.
38. Grabundzija,I., Irgang,M., Mates,L., Belay,E., Matrai,J., Gogol-Doring,A., Kawakami,K., Chen,W., Ruiz,P., Chuah,M.K. *et al.* (2010) Comparative analysis of transposable element vector systems in human cells. *Mol. Ther.*, **18**, 1200–1209.
39. Ammar,I., Gogol-Doring,A., Miskey,C., Chen,W., Cathomen,T., Izsvak,Z. and Ivics,Z. (2012) Retargeting transposon insertions by the adeno-associated virus Rep protein. *Nucleic Acids Res.*, **40**, 6693–6712.
40. Cadinanos,J. and Bradley,A. (2007) Generation of an inducible and optimized piggyBac transposon system. *Nucleic Acids Res.*, **35**, e87.
41. Moldt,B., Yant,S.R., Andersen,P.R., Kay,M.A. and Mikkelsen,J.G. (2007) Cis-acting gene regulatory activities in the terminal regions of sleeping beauty DNA transposon-based vectors. *Hum. Gene Ther.*, **18**, 1193–1204.
42. Walisko,O., Schorn,A., Rolfs,F., Devaraj,A., Miskey,C., Izsvak,Z. and Ivics,Z. (2008) Transcriptional activities of the Sleeping Beauty transposon and shielding its genetic cargo with insulators. *Mol. Ther.*, **16**, 359–369.
43. Newman,J.C., Bailey,A.D., Fan,H.Y., Pavelitz,T. and Weiner,A.M. (2008) An abundant evolutionarily conserved CSB-PiggyBac fusion protein expressed in Cockayne syndrome. *PLoS Genet.*, **4**, e1000031.
44. Baker,M. (2009) Stem cells: fast and furious. *Nature*, **458**, 962–965.
45. Szymczak,A.L., Workman,C.J., Wang,Y., Vignali,K.M., Dilioglou,S., Vanin,E.F. and Vignali,D.A. (2004) Correction of multi-gene deficiency in vivo using a single 'self-cleaving' 2A peptide-based retroviral vector. *Nat. Biotechnol.*, **22**, 589–594.
46. Hotta,A., Cheung,A.Y., Farra,N., Vijayaragavan,K., Seguin,C.A., Draper,J.S., Pasceri,P., Maksakova,I.A., Mager,D.L., Rossant,J. *et al.* (2009) Isolation of human iPS cells using EOS lentiviral vectors to select for pluripotency. *Nat. Methods*, **6**, 370–376.
47. Szabo,P.E., Hubner,K., Scholer,H. and Mann,J.R. (2002) Allele-specific expression of imprinted genes in mouse migratory primordial germ cells. *Mech. Dev.*, **115**, 157–160.
48. Sheridan,S.D., Surampudi,V. and Rao,R.R. (2012) Analysis of embryoid bodies derived from human induced pluripotent stem cells as a means to assess pluripotency. *Stem Cells Int.*, **2012**, 738910.
49. Yoshimizu,T., Sugiyama,N., De Felice,M., Yeom,Y.I., Ohbo,K., Masuko,K., Obinata,M., Abe,K., Scholer,H.R. and Matsui,Y. (1999) Germline-specific expression of the Oct-4/green fluorescent protein (GFP) transgene in mice. *Dev. Growth Differ.*, **41**, 675–684.
50. Huangfu,D., Maehr,R., Guo,W., Eijkelenboom,A., Snitow,M., Chen,A.E. and Melton,D.A. (2008) Induction of pluripotent stem cells by defined factors is greatly improved by small-molecule compounds. *Nat. Biotechnol.*, **26**, 795–797.
51. Garrels,W., Mates,L., Holler,S., Dalda,A., Taylor,U., Petersen,B., Niemann,H., Izsvak,Z., Ivics,Z. and Kues,W.A. Germline transgenic pigs by Sleeping Beauty transposition in porcine zygotes and targeted integration in the pig genome. *PloS One*, **6**, e23573.
52. Maksakova,I.A. and Mager,D.L. (2005) Transcriptional regulation of early transposon elements, an active family of mouse long terminal repeat retrotransposons. *J. Virol.*, **79**, 13865–13874.
53. Subramanyam,D., Lamouille,S., Judson,R.L., Liu,J.Y., Bucay,N., Derynck,R. and Blelloch,R. (2011) Multiple targets of miR-302 and miR-372 promote reprogramming of human fibroblasts to induced pluripotent stem cells. *Nat. Biotechnol.*, **29**, 443–448.
54. Chin,M.H., Mason,M.J., Xie,W., Volinia,S., Singer,M., Peterson,C., Ambartsumyan,G., Aimiuwu,O., Richter,L., Zhang,J. *et al.* (2009) Induced pluripotent stem cells and embryonic stem cells are distinguished by gene expression signatures. *Cell Stem Cell*, **5**, 111–123.
55. Dimos,J.T., Rodolfa,K.T., Niakan,K.K., Weisenthal,L.M., Mitsumoto,H., Chung,W., Croft,G.F., Saphier,G., Leibel,R., Goland,R. *et al.* (2008) Induced pluripotent stem cells generated from patients with ALS can be differentiated into motor neurons. *Science*, **321**, 1218–1221.
56. Ebert,A.D., Yu,J., Rose,F.F. Jr, Mattis,V.B., Lorson,C.L., Thomson,J.A. and Svendsen,C.N. (2009) Induced pluripotent stem cells from a spinal muscular atrophy patient. *Nature*, **457**, 277–280.
57. Xue,X., Huang,X., Nodland,S.E., Mates,L., Ma,L., Izsvak,Z., Ivics,Z., LeBien,T.W., McIvor,R.S., Wagner,J.E. *et al.* (2009) Stable gene transfer and expression in cord blood-derived CD34+ hematopoietic stem and progenitor cells by a hyperactive Sleeping Beauty transposon system. *Blood*, **114**, 1319–1330.
58. Hackett,P.B., Largaespada,D.A. and Cooper,L.J. (2010) A transposon and transposase system for human application. *Mol. Ther.*, **18**, 674–683.
59. Belay,E., Matrai,J., Acosta-Sanchez,A., Ma,L., Quattrocelli,M., Mates,L., Sancho-Bru,P., Geraerts,M., Yan,B., Vermeesch,J. *et al.* (2010) Novel hyperactive transposons for genetic modification of induced pluripotent and adult stem cells: a nonviral paradigm for coaxed differentiation. *Stem Cells*, **28**, 1760–1771.
60. Jin,Z., Maiti,S., Huls,H., Singh,H., Olivares,S., Mates,L., Izsvak,Z., Ivics,Z., Lee,D.A., Champlin,R.E. *et al.* (2011) The hyperactive Sleeping Beauty transposase SB100X improves the genetic modification of T cells to express a chimeric antigen receptor. *Gene Ther.*, **18**, 849–856.
61. Wang,Y., Chen,J., Hu,J.L., Wei,X.X., Qin,D., Gao,J., Zhang,L., Jiang,J., Li,J.S., Liu,J. *et al.* (2011) Reprogramming of mouse and human somatic cells by high-performance engineered factors. *EMBO Rep.*, **12**, 373–378.

62. Qiu,C., Ma,Y., Wang,J., Peng,S. and Huang,Y. (2010) Lin28-mediated post-transcriptional regulation of Oct4 expression in human embryonic stem cells. *Nucleic Acids Res.*, **38**, 1240–1248.
63. Warlich,E., Kuehle,J., Cantz,T., Brugman,M.H., Maetzig,T., Galla,M., Filipczyk,A.A., Halle,S., Klump,H., Scholer,H.R. *et al.* (2011) Lentiviral vector design and imaging approaches to visualize the early stages of cellular reprogramming. *Mol. Ther.*, **19**, 782–789.
64. Kim,H., Lee,G., Ganat,Y., Papapetrou,E.P., Lipchina,I., Socci,N.D., Sadelain,M. and Studer,L. (2011) miR-371-3 expression predicts neural differentiation propensity in human pluripotent stem cells. *Cell Stem Cell*, **8**, 695–706.
65. Li,Z., Yang,C.S., Nakashima,K. and Rana,T.M. (2011) Small RNA-mediated regulation of iPS cell generation. *EMBO J.*, **30**, 823–834.
66. Lipchina,I., Elkabetz,Y., Hafner,M., Sheridan,R., Mihailovic,A., Tuschl,T., Sander,C., Studer,L. and Betel,D. (2011) Genome-wide identification of microRNA targets in human ES cells reveals a role for miR-302 in modulating BMP response. *Genes Dev.*, **25**, 2173–2186.
67. Leung,A.K., Young,A.G., Bhutkar,A., Zheng,G.X., Bosson,A.D., Nielsen,C.B. and Sharp,P.A. (2011) Genome-wide identification of Ago2 binding sites from mouse embryonic stem cells with and without mature microRNAs. *Nat. Struct. Mol. Biol.*, **18**, 237–244.
68. Tesar,P.J., Chenoweth,J.G., Brook,F.A., Davies,T.J., Evans,E.P., Mack,D.L., Gardner,R.L. and McKay,R.D. (2007) New cell lines from mouse epiblast share defining features with human embryonic stem cells. *Nature*, **448**, 196–199.
69. Brons,I.G., Smithers,L.E., Trotter,M.W., Rugg-Gunn,P., Sun,B., Chuva de Sousa Lopes,S.M., Howlett,S.K., Clarkson,A., Ahrlund-Richter,L., Pedersen,R.A. *et al.* (2007) Derivation of pluripotent epiblast stem cells from mammalian embryos. *Nature*, **448**, 191–195.
70. Nichols,J. and Smith,A. (2009) Naive and primed pluripotent states. *Cell Stem Cell*, **4**, 487–492.
71. Jouneau,A., Ciaudo,C., Sismeiro,O., Brochard,V., Jouneau,L., Vandormael-Pournin,S., Coppee,J.Y., Zhou,Q., Heard,E., Antoniewski,C. *et al.* (2012) Naive and primed murine pluripotent stem cells have distinct miRNA expression profiles. *RNA*, **18**, 253–264.